2015-01-01

High Temperature Helical Tubular Receiver For Concentrating Solar Power System

Nazmul Hossain
University of Texas at El Paso, nhossain@miners.utep.edu

HIGH TEMPERATURE HELICAL TUBULAR RECEIVER FOR CONCENTRATING SOLAR POWER SYSTEM

NAZMUL HOSSAIN

Master's Program in Computational Science

APPROVED:

Vinod Kumar, Ph.D., Chair

Shirley Moore, Ph.D.

Pavana Prabhakar, Ph.D.

Norman Love, Ph.D.

Charles Ambler, Ph.D.
Dean of the Graduate School

Dedication

To my parents, and sisters who have been supporting me unconditionally, and be there for me whenever I needed. To the rest of my family and friends, thanks for always supporting me and being there for me.

HIGH TEMPERATURE HELICAL TUBULAR RECEIVER FOR CONCENTRATING SOLAR POWER SYSTEM

by

NAZMUL HOSSAIN, B.Sc.ME

THESIS

Presented to the Faculty of the Graduate School of

The University of Texas at El Paso

in Partial Fulfillment

of the Requirements

for the Degree of

MASTER OF SCIENCE

Computational Science Program

THE UNIVERSITY OF TEXAS AT EL PASO

August 2015

Acknowledgements

I would like to show my deepest gratitude to all my family members, especially my parents and my sister. They have always been there for me, when I needed them. Your encouragement and support have been the key for me to accomplish my goals.

My biggest appreciation goes to my mentor and committee chair Dr. Vinod Kumar to give me the opportunity to work with him in Computational Fluid Dynamics lab. His guidance with knowledge and experience motivated me in moving forward to achieve my goals. His excellent mentorship and encouragement helped me to complete research projects and grow as a future researcher. It was a pleasure to work under his mentorship.

I am thankful to Dr. Shirley Moore, Dr. Pavana Prabhakar and Dr. Norman Love for agreeing to serve on my thesis committee and providing me with the mentorship and encouragement to complete this work. I am also very grateful to all the members of Computation Science Program, especially Dr. Ming-Ying Leung and Cindy Davis for their support and guidance.

I also gratefully acknowledge the co-operation and all the help of all my friends and research colleagues, especially Samia Afrin, Jesus Ortega and my mentoring group.

Abstract

In the field of conventional cleaner power generation technology, concentrating solar power systems have introduced remarkable opportunity. In a solar power tower, solar energy concentrated by the heliostats at a single point produces very high temperature. Falling solid particles or heat transfer fluid passing through that high temperature region absorbs heat to generate electricity. Increasing the residence time will result in more heat gain and increase efficiency. A novel design of solar receiver for both fluid and solid particle is approached in this paper which can increase residence time resulting in higher temperature gain in one cycle compared to conventional receivers. The helical tubular solar receiver placed at the focused sunlight region meets the higher outlet temperature and efficiency. A vertical tubular receiver is modeled and analyzed for single phase flow with molten salt as heat transfer fluid and alloy625 as heat transfer material. The result is compared to a journal paper of similar numerical and experimental setup for validating our modeling. New types of helical tubular solar receivers are modeled and analyzed with heat transfer fluid turbulent flow in single phase, and granular particle and air plug flow in multiphase to observe the temperature rise in one cyclic operation. The Discrete Ordinate radiation model is used for numerical analysis with simulation software Ansys Fluent 15.0. The Eulerian granular multiphase model is used for multiphase flow. Applying the same modeling parameters and boundary conditions, the results of vertical and helical receivers are compared. With a helical receiver, higher temperature gain of heat transfer fluid is achieved in one cycle for both single phase and multiphase flow compared to the vertical receiver. Performance is also observed by varying dimension of helical receiver.

Table of Contents

List of Tables

List of Figures

Chapter 1: Introduction

With rising demand for energy, scientists and engineers are looking for efficient ways of power generation from cleaner energy sources to ensure a sustainable future. More than 60% of our supplied energy is generated by burning fossil fuels [1]. This burning of fossil fuels lead to enormous amount of CO_2 emission, which is the major cause of greenhouse effect. The greenhouse effect eventually leads to global warming and climate disasters throughout the world. I order to escape from this viral situation, we need a cleaner abundant source of power supply and that's where renewables are more dependable. Among renewable energy sources, solar energy is the most promising, cleaner, abundant and available source of energy. Solar energy is being utilized using photovoltaic and CSP technologies. Photovoltaic system is limited to low temperature and uses batteries in order to have a continuous supply of energy, which is chemically toxic and very expensive. However, with CSP, very high temperature may be achieved and with the addition of thermal storage system, it provides promising performance.

Concentrating Solar Power (CSP) technology has introduced a potential power generation technique supplemented with an energy storage system. Unlike Concentrated Photovoltaic (CPV), CSP plant with thermal storage system can generate power when the sun is not available. In CSP plants, focused sunlight from heliostats provides a very high temperature at a small region. Heat gain by the heat transfer fluid at that region determines the performance.

Recent central solar receiver technologies can reach up to 600^{o}C using either steam or molten nitrate salt as the heat transfer fluid (HTF) [2][3]. Above 600^{o}C molten nitrate salt becomes unstable and a shortcoming of steam as HTF is its low heat transfer capacity [2], [3]. Suitable HTF's can reduce the costs and size and also increase power cycle efficiencies. Hence, electricity generation from a CSP power plant is expected to be cost competitive with conventional power generation systems and to meet or surpass the DOE's SunShot target of 6¢/kWh. In order to achieve this goal, we need to develop novel high temperature HTF and efficient high temperature solar receiver. To overcome this issue, direct absorption receivers

using solid particles as the heat transfer medium (HTM) become an alternative option. The National Renewable Energy Laboratory has proposed a near black body falling particle receiver with 85% efficiency, and Sandia National Laboratories is developing a prototype of a curtain shape falling particle receiver with their facility [4].

The challenge of this curtain shape falling particle receiver is to reach a certain high temperature. As the residence time of HTF is very small, it is important to maximize the residence time, so that sufficient heat absorption will occur at the concentrated beam region and the required HTF temperature can be achieved in one cyclic operation. Also, because of increased residence time, the required HTF temperature may be achieved with lower heat flux at the concentrated region. This may lead to using fewer heliostats and generating electricity with conventional source in a more cost competitive way.

This thesis has been divided into several chapters. A brief introduction of the importance of solar energy technology and the development in concentrating solar power are discussed in Chapter 1. In Chapter 2, literature reviews on total energy production, availability and demand throughout the world are mentioned. The literature is focused on renewables, solar energy and concentrating solar power technology. The recent advancements in these sectors and growth rate of renewables and CSP technology in recent years have been highlighted. The case study considered for the thesis is described in chapter 3. The methods used to solve problems are also explained in this chapter for single phase and multiphase flow with computational modeling. Numerical results from the simulations are shown and discussed in chapter 4. Finally, we conclude with the summary of results and future work in chapter 5 and chapter 6, respectively.

Chapter 2: Background and Literature Review

We are living in a world with constant increase in consumption of energy. Our primary source of providing this huge amount of energy is fossil fuels. Earth has limited amount of these resources and with vast amount of energy demand, these resources are slowly becoming scarce. Every year, energy demand has been increasing throughout the world. Regional energy consumption of the world from 1971 to 2012 is shown in figure 2.1.

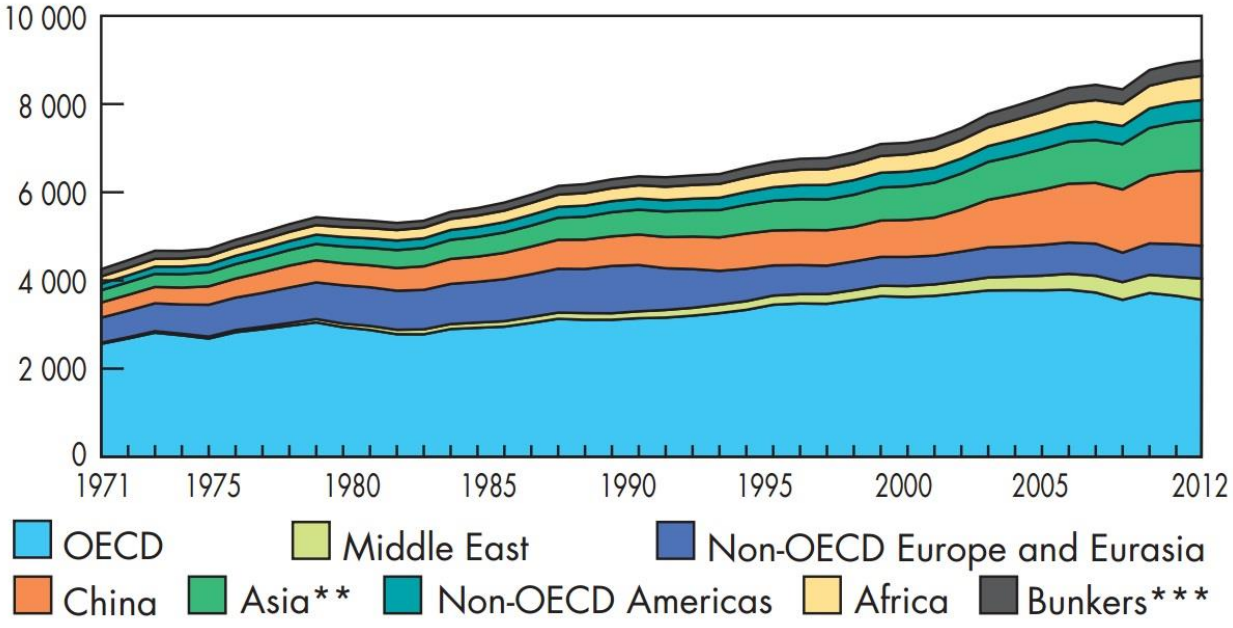

Figure 2.1: World total energy consumption from 1971 to 2012 by region (Mtoe)[35]

Fossil fuel such as petroleum, natural gas, and coal has been the main source to meet this high energy demand as shown in figure 2.2. It causes carbon dioxide and other toxic gas emission, which is assumed to be a major cause of global warming [5]. Only in year 2012, approximately 21532 Billion KWh electricity is generated throughout the world and about 67.33% of that is produced by burning fossil fuels [6]. Approximately 21310 Million Metric Tons of CO_2 is emitted by burning of this fossil fuels, which is 155 million metric tons more

from the previous year [6]. In order to overcome the situation CO_2 emission limitations have been proposed [7].

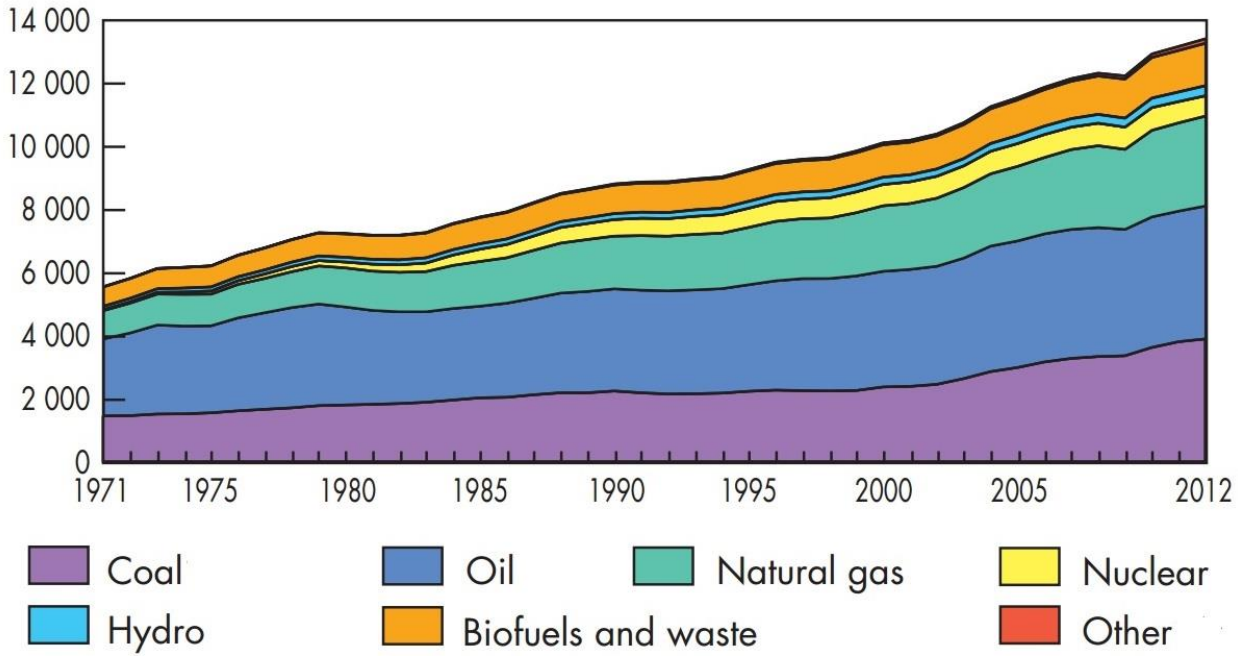

Figure 2.2: World total energy supply from 1971 to 2012
by fuel (Mtoe)[35]

United States overall energy consumption grew to 97.3 quadrillion Btu in 2013, which is a 2.4% increase from 2012. Energy consumption from coal and renewables grew slightly while consumption from petroleum and natural gas fell slightly [8]. Dependence on the environment, low capacity power generation and large capital cost have been the obstacles to renewable energy. With development of modern technology, we are gradually advancing to overcome these problems. There have been many developing technologies of energy storage system [9]–[17]. Renewable electricity grew to nearly 15% of total installed capacity and 13% of total electricity generation in the United States in 2013. Installed renewable electricity capacity exceeded 171 GW in 2013, generating 534 TWh [8].

2.1 RENEWABLE ENERGY

In the field of renewable energy, natural resources that do not diminish over time are sources of power generation. Hydropower, wind, solar, geothermal, biofuel are sources of renewable energy. These resources are widely available and considered to be clean sources of energy, which are environmental friendly.

Hydropower is a very potential source of renewables for power generation. It is the largest source of renewable energy. Approximately 16% of world's total energy was produced from hydropower by the end of 2008 [18]. It utilizes water at an elevated position to generate electricity. Wind power is another source of renewables, which utilized the wind to generate electricity. Approximately 0.8% of world's total energy was produced from wind energy by the end of year 2009 [19]. There is also geothermal energy, which utilizes energy stored in earth and bio energy, which utilizes organic material to extract the chemical energy.

All of the renewable energy sources mentioned, depends on certain conditions, like the hydropower is depended on elevated water. So, these sources are not available everywhere. However, solar energy or the solar radiation from the sun is available every corner of the world. Amount of energy consumed in the world is only $1/10000^{th}$ energy from the sun [20]. Less than 0.5% of this vast resource was being utilized by 2012 [6]. This the most available and largest clean energy source that can provide our growing energy demand and promise a clean environment for our future.

2.2 SOLAR TECHNOLOGIES

Solar energy is the most available clean source of energy. An enormous amount energy is emitted from the sun and a fraction of that energy reaches earth's atmosphere. Solar energy reaching our atmosphere is considered to be between 1353 W/m2 to 1395 W/m2, which is approximately 1.4 KW/m2 [21]. Solar energy can provide us 25000 times the total energy used from all other sources [22]. However, only a little fraction of this vast amount of energy is being

utilized. With the current global energy consumption rate and gradual decrease in fossil fuel, solar energy has the potential to become the future of fulfilling global energy demand. Solar technology may provide us with the solution of clean energy source that we have been striving for. We have been introduced to different technologies for harnessing solar radiation. Among solar technologies, Photovoltaic cells and Concentrating solar power technology have been most promising as an alternative to electric power generation from fossil fuels. Utilization of solar energy instead of other renewables is so much more important, because of the availability throughout the world.

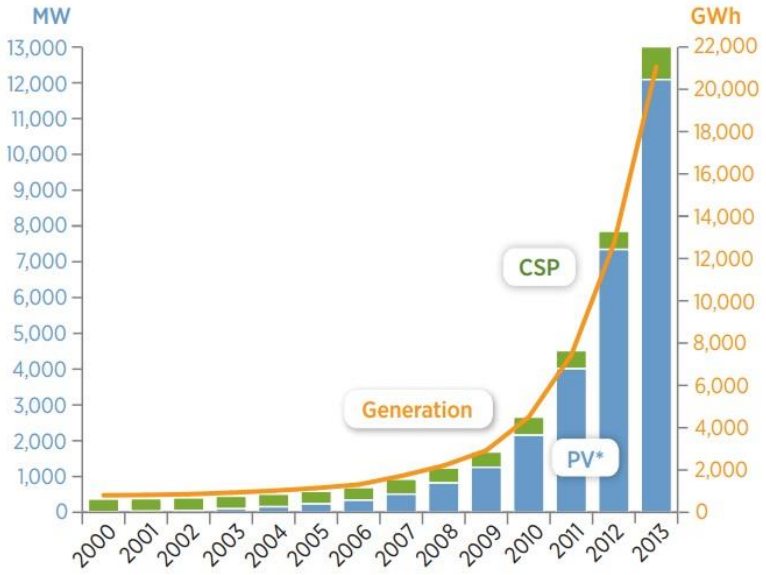

	U.S. Solar Energy Generation (GWh)	U.S. Solar Energy Capacity (MW) and % Increase from Previous Year			
		PV*	CSP	Total	Increase
2000	804	18	354	372	4.3%
2001	822	29	354	383	3.0%
2002	857	52	354	406	5.9%
2003	929	97	354	451	11.2%
2004	1,020	155	354	509	12.8%
2005	1,145	234	354	588	15.5%
2006	1,312	339	355	694	18.0%
2007	1,718	508	419	927	33.5%
2008	2,208	819	419	1,237	33.5%
2009	2,923	1,257	430	1,687	36.3%
2010	4,507	2,153	508	2,661	57.7%
2011	7,437	4,011	508	4,519	69.8%
2012	12,692	7,344	508	7,852	73.8%
2013	21,074	12,090	918	13,008	65.7%

Figure 2.3: Total solar electricity installed capacity and generation in United States [8]

In photovoltaic cells solar technology, silicon semiconductors are used to convert solar radiation or photons into electrons by photovoltaic effect. This physical and chemical phenomenon leads to generating electricity with solar cells while exposed to sunlight. With the accumulation of a large number of solar cells, a utility-scale PV system is developed. Solar electricity generation capacity grew by a factor of 35 between 2000 to 2013 and currently accounts for 0.5% of annual electricity generation. PV cumulative capacity increased 65% in 2013 alone [8].

Concentrating solar power technology has become one of the best solar energy utilization process for providing large power supply. In CSP technology, sunlight from a large area is focused into one point using mirrors to achieve very high temperature region. While passing through that high temperature region, the heat transfer fluid gains heat and then converts this heat energy into electricity by passing steam through turbine. The major drawback of solar energy technology was the inconsistent supply of solar radiation because of night time and weather conditions. The addition of thermal storage system to CSP technology has opened a new door for us. Using thermal storage to store heat, now we can provide a constant supply of electricity overcoming the drawback. Now, electricity production in commercial scale is easily possible utilizing thermal storage to store heat and generate power, whenever necessary. There have been several CSP plant active throughout the world. 410 MW of new CSP capacity came online in the United States in 2013, which is an increase in cumulative capacity of 81%. Approximately 400 MW to 500 MW of CSP capacity is currently under construction and expected to come online soon, while another 3600 MW is under development [8].

2.3 CONCENTRATING SOLAR POWER SYSTEM

In a CSP system, solar radiation is accumulated from a large area and focused in one region to have a high temperature region. Heat transfer fluid is passed through that region to capture the heat energy and convert it to electricity. There have been 3 different approaches to utilize CSP technologies.

1. Trough System
2. Dish/ Engine System
3. Solar Power Tower System

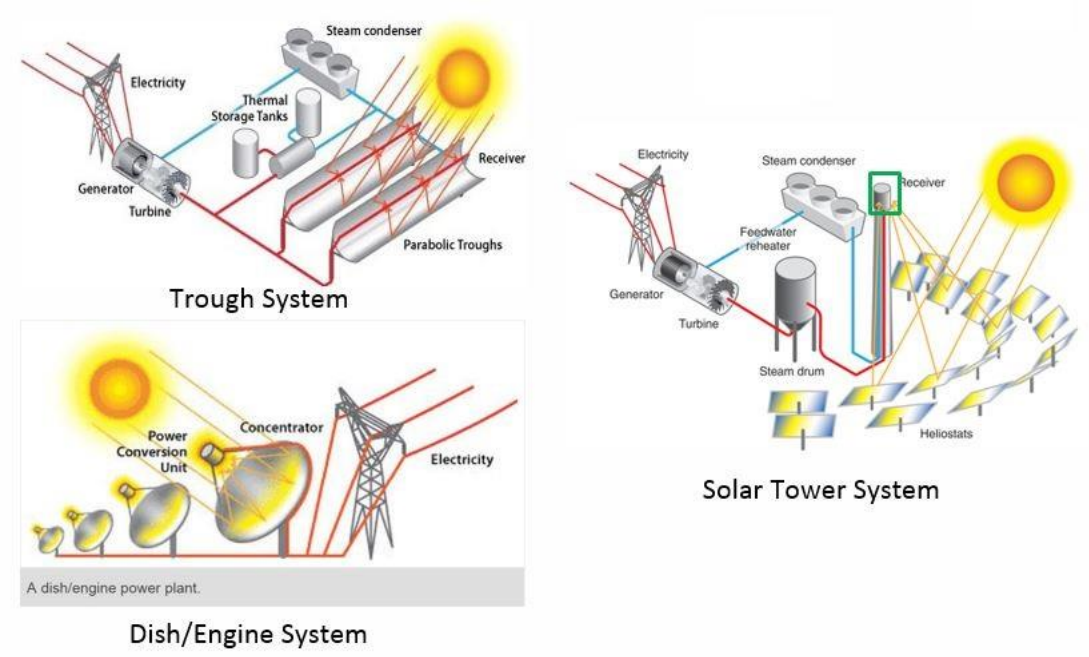

Figure 2.4: CSP systems schematic diagram [36] [37] [38]

Though system in CSP absorbs solar energy by using long rectangular or parabolic trough collectors. The trough collectors are positioned across the north-south axis. Receiver tubes are positioned along the focal line of parabolic troughs. The troughs move along east to west axis gradually with the sun to collect solar radiation properly. The reflected solar radiation from parabolic trough to receiver generates very high temperature (about 550^{o} C). Fluid passing through that receiver absorbs the heat energy and convert it to electricity with the help of a turbine. A schematic of a parabolic trough system is shown in figure 2.3.

A parabolic dish of mirrors is used to concentrate solar radiation at the focal point in a dish/ engine system. The solar concentrator and the power conversion unit are the two major parts in this system. The solar concentrator is the dish, which rotates with the sun throughout the day to get maximum radiation. The conversion unit includes thermal receiver and engine. Heat energy is received by the receiver and converted to power with the engine. With this technology,

a small amount of electricity is produced compared to other CSP technologies. A schematic of a dish/ engine CSP system is shown in figure 2.4.

In a concentrated solar power tower, sunlight from a large area is accumulated by using heliostats or flat mirrors. Using the mirrors, solar radiation is focused on a receiver on top of a centrally located tower. At that critical region, very high temperature ($500^oC\ to\ 1200^oC$) can be achieved [4]. Water is passed through that high temperature region to generate steam for turbine to convert the heat energy to electricity, or other heat storage material like molten salt, sand particles etc. can be used to store the absorbed heat so that it may be used to generate power later. A schematic diagram of solar power tower with thermal storage system is shown in figure 2.3.

The first commercial solar power tower known as PS0 was built by Abengoa Solar of Spain in the Spanish province of Seville. It began operation in March, 2007 and continues to this day [23]. One of the largest solar tower systems located across 3,500 acres of federal land in California's Mojave Desert is known as the Ivanpah facility. It is a 392 MW CSP plant consisting of 173,500 heliostats and three power towers with the capacity to provide clean, sustainable energy to over 100,000 American homes [24].

Solar collectors capture solar radiation by reflecting focused sunlight to the receiver, thus creating heat energy to generate electricity. About 40% of the total system cost is for collectors. In reducing power generation cost with CSP technology, developing low cost, high performance and highly durable collector design plays a vital role. Soiling of the solar collectors may lead to 8% to 12% drop in performance during cleaning. Also, cleaning may become a big problem in deploying massive scale CSP plant in low water desert areas. Researchers have been working on developing a lower cost, long-term durable and cleanable solar collector to improve performance of the overall system. Currently, they are trying to develop reflectors maintaining more than 95% specular resistance for over 30 years under harsh environment.

2.4 THERMAL STORAGE

The solar energy system has faced numerous challenges. Among them the most accumulating challenge is reduced or curtailed energy production when the main power source (sun) sets or it is obstructed by clouds. To overcome this problem, Scientist come up with a solution named Thermal Energy Storage or TES. Thermal energy storage systems mainly consist of high pressure liquid storage tanks which allow to store several hours of electricity.

Many systems have been tested for the TES technologies since the first solar thermal power plants were constructed in 1980. After evaluation and testing, developers of these systems came up with the three possible solutions. These are: a two tank direct system, a two tank indirect system, and a single tank thermocline system.

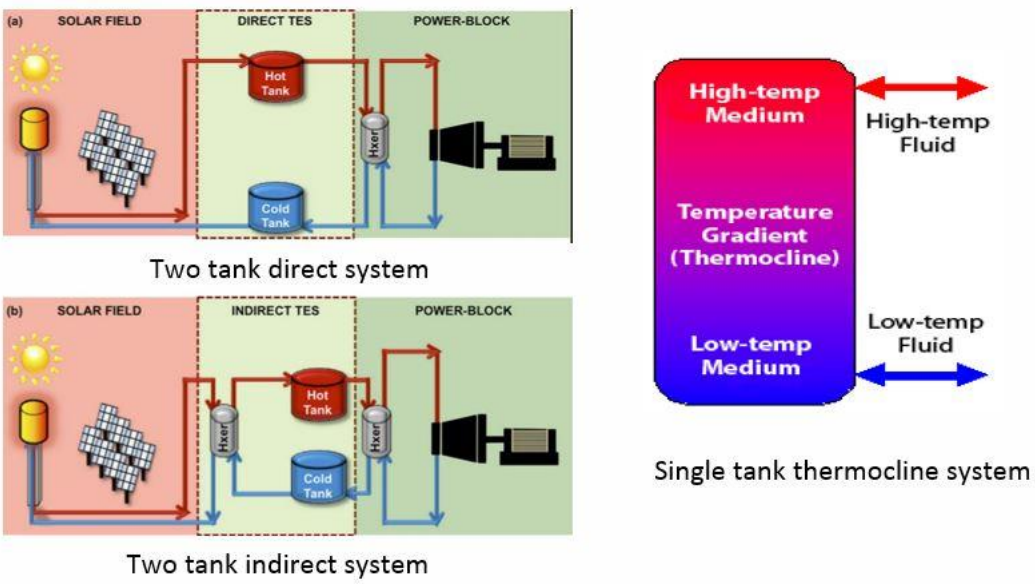

Figure 2.5: Thermal storage systems schematic diagram [39] [40]

In this system, the storing fluid and the working fluid are same. The fluid is stored in two tanks, one of low temperature and one of high temperature. The fluid is transferred from the low temperature tank to the solar collector or receiver, where it gets hot by the heat provided by the solar energy. After that, it circulates to the high temperature tank for storage. After passing

through a heat exchanger, the cooled fluid drifts back to the low-temperature tank to be reused. For the heat transfer fluid, molten salt or synthetic oil has been used in this system.

Two tank indirect system is same as two tank direct system except for the using of the fluids. This system uses different fluids for storing and heat transfer. This system is mainly used in plants where the heat transfer fluid is too costly or not appropriate for both of the fluids. This system requires an extra heat exchanger, which leads to extra cost to the total system. In these systems, the storage fluid which originates from the low tank temperature flows through an extra heat exchanger. The heat exchanger gets heated from the heat transfer fluid. After getting hot, the storage fluid get backs to the high temperature storage tank and on the other hand, the low temperature HTF goes to the solar collector or receiver to get heated again and does the process repeatedly.

Apart from the above mentioned two systems, there exists another system called single tank thermocline system, in which the system stores the thermal energy in a solid medium. The medium which is mostly used is silica sand or concrete. The reason for inventing this system is for reducing the cost of the storage fluid and the tanks, and this system fulfilled this criteria very well. Inside the single tank, parts of the solid are kept at low to high temperatures, in a temperature gradient, depending on the flow of fluid. For storing, hot heat-transfer fluid flows into the top of the tank and cools as it travels down, exiting as a low temperature liquid. To generate steam and produce electricity, the process is reversed. Buoyancy effects produce thermal stratification of the fluid within the tank, which helps to alleviate and sustain the thermocline.

2.5 SOLAR TOWER RECEIVERS

In a CSP plant, sunlight is focused on the receiver to absorb heat energy for the power generation process. Different types of receivers have been introduced and experimented with to achieve best performance in CSP power generation technique. There have been cavity type, tubular, serpentine, curtain shape, and ceramic plate with different panel arrangements and

volumetric receivers. In power plant Julich (DLR), with open volumetric air receivers, 680^oC outlet temperature is achieved for 120^oC inlet at ambient pressure [25]. EU-project under Abengoa Solar NT tested 3MW metallic tubular receiver and was able to achieve from 330^oC inlet temperature to 800^oC outlet temperature at 10 bar pressure [26]. In ceramic plate receivers, mass flow is distributed to a number of parallel receivers. The absorber tubes have small diameters for better heat transfer with various panel arrangements. There have been some work with the following type of receivers.

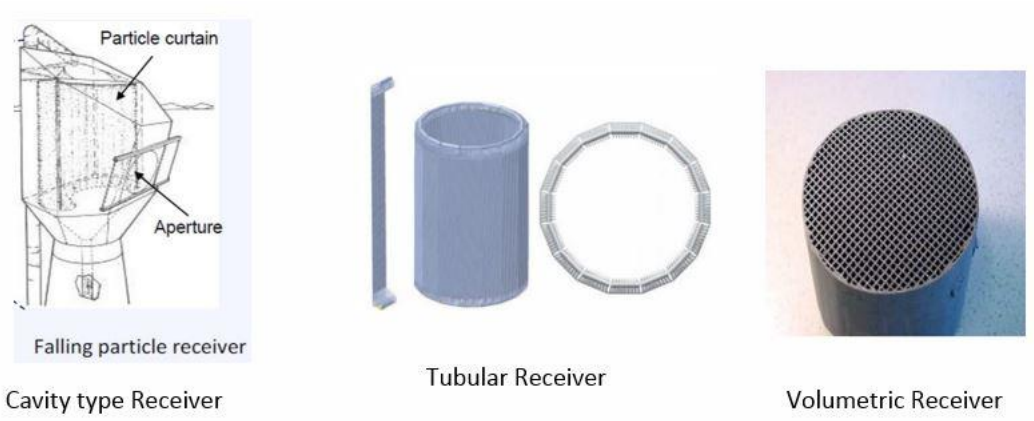

Figure 2.6: CSP solar tower receivers [41][42][25]

The cavity type receiver is used for solid particle heat transfer fluid. A curtain of solid particle is dropped from top and concentrated heat flux directly passed through the curtain for the solid particles to achieve a very high temperature immediately. Sand, boxite, alumina and several other potential high heat capacity solid particle is being analyzed for this type of receiver.

Tubular receiver is used in most of the operating solar tower plant. Vertical tube arrangement is set up and heat transfer fluid is passed through the tubes in the high temperature region to absorb heat energy. Molten salt is mostly used as heat transfer fluid in this type of receiver system.

In volumetric receiver, the high temperature region is made porous so that it will take more time the heat transfer fluid to pass through the region and absorb more heat in just one cycle. Compressed air and supercritical CO_2 are potential heat transfer fuid for this type of receiver system.

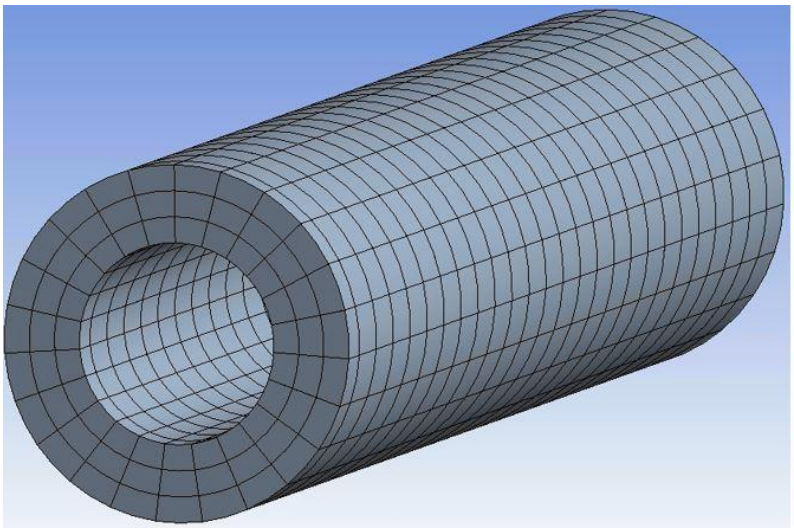

Figure 2.7: High temperature & pressure direct tubular receiver [43]

High temperature and pressure tubular receiver using supercritical CO_2 has been analyzed by one of our group member Jesus Ortega. His designed receiver has about 10 mm thickness to withstand the high internal pressure developed by supercritical CO_2. Figure 2.7 shows a diagram of his designed vertical tubular receiver. A new type of tubular receiver was introduced by another of our group member, Samia Afrin. She designed a serpentine tubular receiver as shown in figure 2.8, coated with Pyromark 2500 using supercritical CO_2 as heat transfer fluid. Pyromark coating was used to reduce the radiative losses for the receiver.

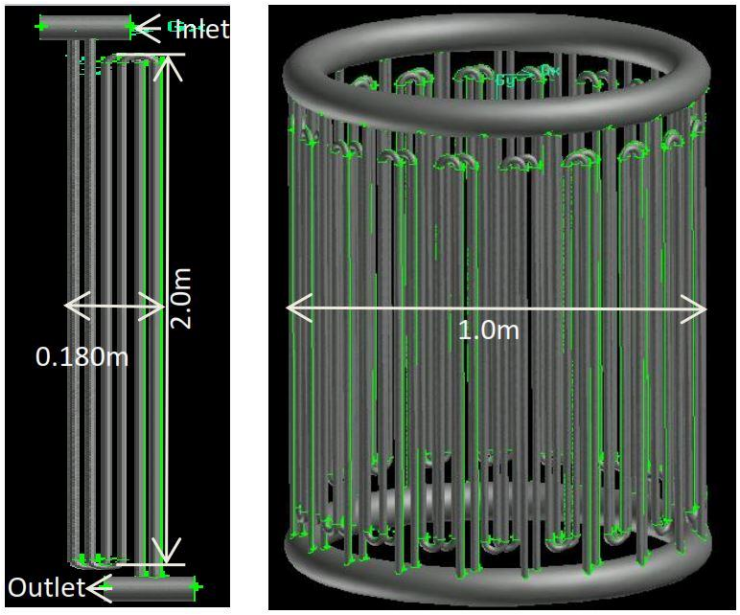

Figure 2.8: Serpentine receiver for solar tower in CSP [33]

Receivers may also be classified by heat transfer medium such as molten salt, water/steam, air open/closed, liquid metals, solid particles and other gases. In the direct storage concept, the heat transfer fluid is also used as the storage medium. In indirect storage, a different storage medium is used. Molten salt has been mostly used in solar tower systems because of its low cost and good heat transfer characteristics. It usually consist of 60% NaNO3 and 40% KNO3 and is used to generate up to 565^oC superheated steam [2][27]. It freezes below 220^oC, which makes it problematic to pump at low temperature. Also, the salt is corrosive and becomes unstable at temperature higher than about 600ºC. There has been testing with solid sand particle in Sandia National Laboratory for a cavity type curtain shape receiver. Different types of ceramic solid particles are being tested as heat transfer and storage medium because of its high temperature durability (>900^oC) and direct absorbing of solar radiation without any limit in heat flux densities. A prototype (10 KW) of centrifugal particle receiver has been successfully tested up to 900^oC. Nanofluidized heat transfer fluid has been developed by nano-particle suspension in molten salt to improve salt performance [28].

Chapter 3: Problem Statement & Methodology

Our study is mainly focused on designing a novel high temperature solar tower receiver. We have designed a receiver so that it may provide better performance than conventional receivers. As the experimental approach is too expensive, we decided to investigate the designed receiver performance through numerical simulation. We also used an experimental approach for validating our modeling results.

Our primary purpose is to increase the residence time of the heat transfer fluid, so that it may have more time to absorb heat energy. A vertical receiver is modeled for single phase in [29], and we compared with our result to validate our modeling. Using the same modeling parameters, a helical shaped tubular receiver is analyzed and compared with a vertical tubular receiver. Also, the number of rotations and diameter of receiver are varied to observe the change in performance of helical receivers.

With the same receivers, a multiphase model is used to analyze solid particle as the heat transfer fluid. Air is used as primary phase and alumina particle is used as secondary phase. Eulerian granular multiphase model is considered for our case problems.

For designing, Solidworks2013 [30] software is used and for simulation, commercial software Ansys FLUENT 15.0 [31] is used. In FLUENT, Eulerian Granular model is considered for multiphase flow and air is used as primary phase. Receiver material is considered as alloy625 and transparent quartz tube for sunlight to pass through. One receiver for validation and four other receivers for result comparison are designed. Also, DO (Discrete Ordinate) radiation model is used to analyze the fluid flow through receiver for better understanding.

3.1 DESIGN

In the design of tubular receiver for solar tower, one of our major concern was to increase the resident time so that the heat transfer fluid will have more time for heat transfer while passing through the high temperature region. Also, we wanted to design a receiver without any sharp edges. The reason behind this, is for the receiver to withstand comparatively high stress

with lower tube thickness, without causing fracture or buckling. The receiver is designed in such a way that the cold HTF will pass through the receiver from inlet to outlet in downward direction. With the downward direction flow, gravitational force will assist the HTF to pass through the receiver. That way, beside fluid, we are also able to consider free falling solid particle for our receiver. A schematic diagram of helical receiver is shown in following figure 3.1.

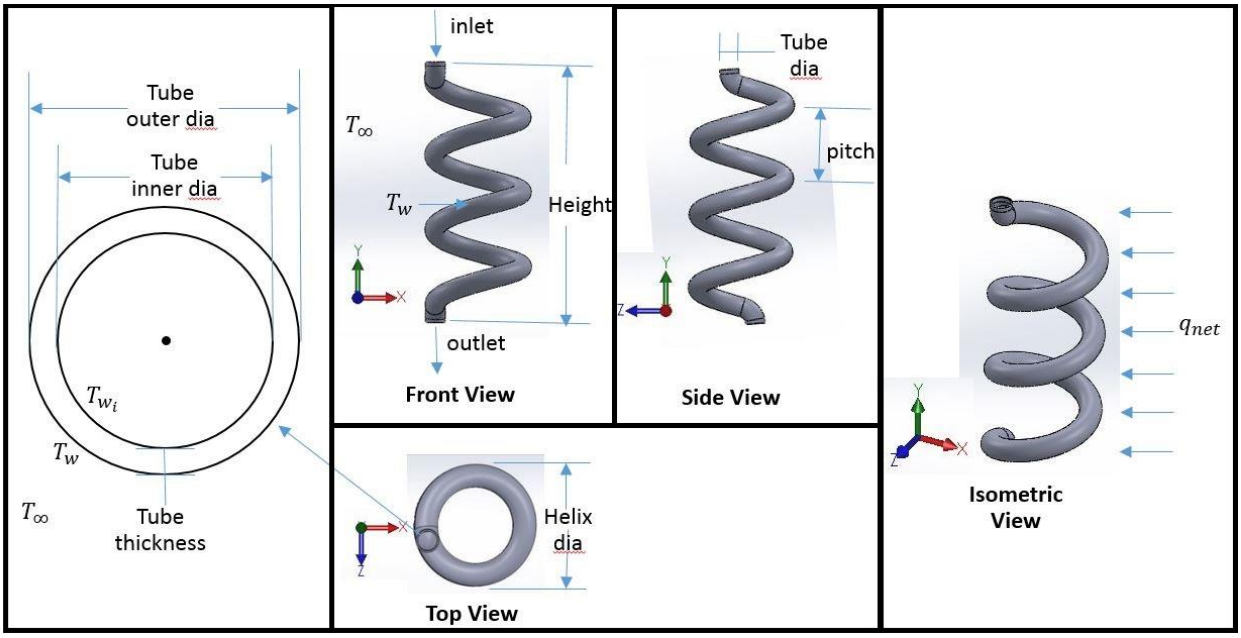

Figure 3.1: Schematic diagram of helical receiver

As we can see from the schematic diagram that the net heat flux is coming from one side of the receiver. T_w and T_∞ are tube wall temperature and ambient temperature respectively. Pitch is the vertical height of one single rotation of helical receiver. The pitch and helix diameter are related to the inclination angle of the receiver. We considered the pitch and helix diameter in such a way that the inclination angle always greater than 30^o for considering free fall of HTF. Complete arrangement of vertical and helical tubular receiver is designed as shown in figure 3.2. A single part of the receivers are analyzed numerically because of the limitation of computational resources.

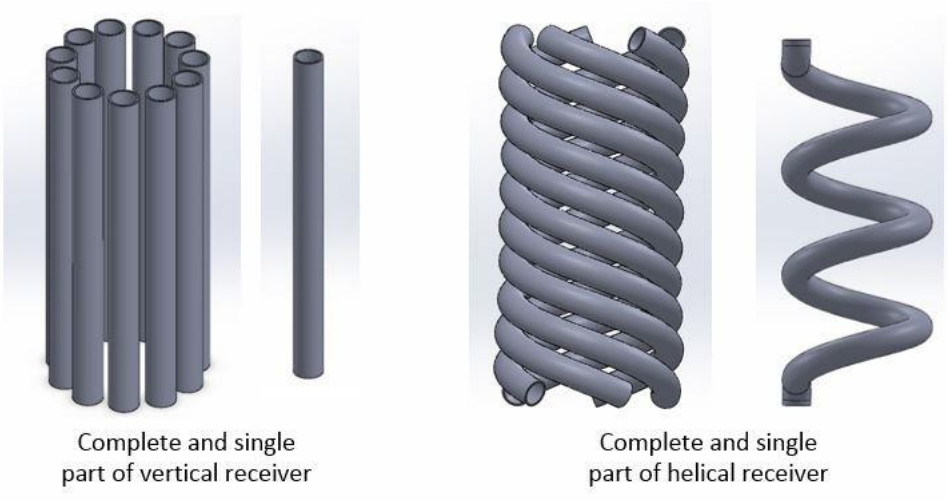

Figure 3.2: Schematic of complete and single part of receivers

The advantage of helical receiver over vertical receiver is that the path is twisted throughout the height. This leads to a higher resident time for HTF in helical receiver. Also, when we stack the helical tubes one after the other, they will support one another operating in high internal pressure and reduce the possibility of buckling according to mechanics of materials. Another advantage of the helical receiver is that the fluid will have swirling effect according to fluid dynamics, while passing through the helical tube. This phenomena will reduce the possibility of obtaining very high temperature in one region and low temperature on the other region of fluid so that HTF limited to a high temperature can be considered for helical receiver. We designed five solar tower receivers for our study. The dimension and arc length of the receivers are shown in Table 3.1. A schematic of the receivers are shown in figure 3.3. Arc length is calculated using equation 1 in following formula [32].

$$Helix\ arc\ length = \sqrt{(\pi DT)^2 + H^2} \quad (1)$$

Here, D = Helix diameter

T = Number of turns

H = Height of receiver

Table 3.1: Height and arc length of receivers

Receiver	tube outer dia (mm)	helix dia (mm)	Height (mm)	Rotation	Arc Length (mm)
R1	20		1000		1000
R2	46		600		600
R3	46	246	600	3	2393.74
R4	46	246	600	2	1657.30
R5	30	230	600	2	1564.06

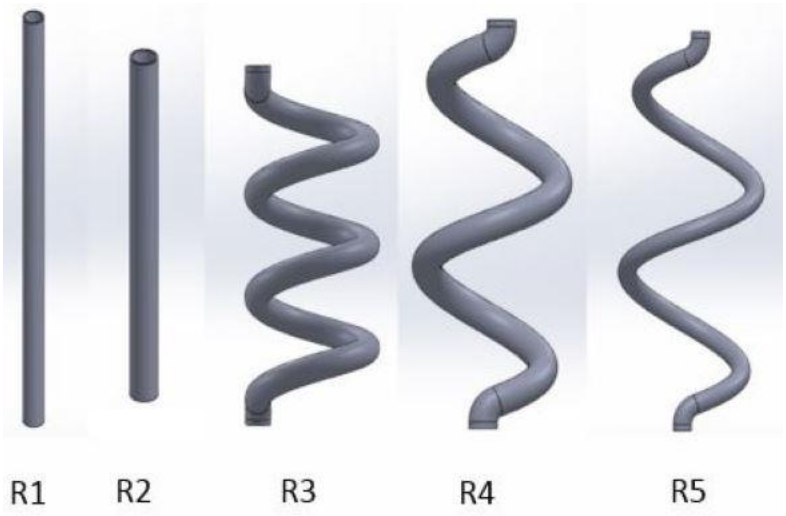

Figure 3.3: Single parts of five designed receivers

From left to right are Receiver 1 to Receiver 5. Receiver 1 is used for modeling validation. Receiver 2 to Receiver 5 have the same vertical height. Receiver 2 is designed to show that with the same vertical height, helical receiver can have a better performance. Receiver 3 to receiver 5 are used to find the optimum characteristics of helical receiver and to determine how the performance varies with the change of pitch and tube diameter.

3.2 MESHING

Ansys CFD mesh modular is used to generate the mesh and divide the receivers into number of elements to apply Finite Volume Method for our numerical study. Inflation is applied on the surface to have better control of the mesh with fewer mesh elements. The total number of mesh elements for all the receivers was kept under 512000.

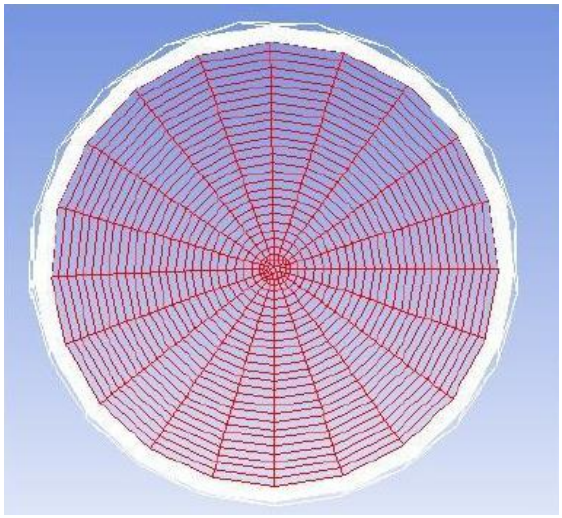

Figure 3.4: Mesh at tube inlet

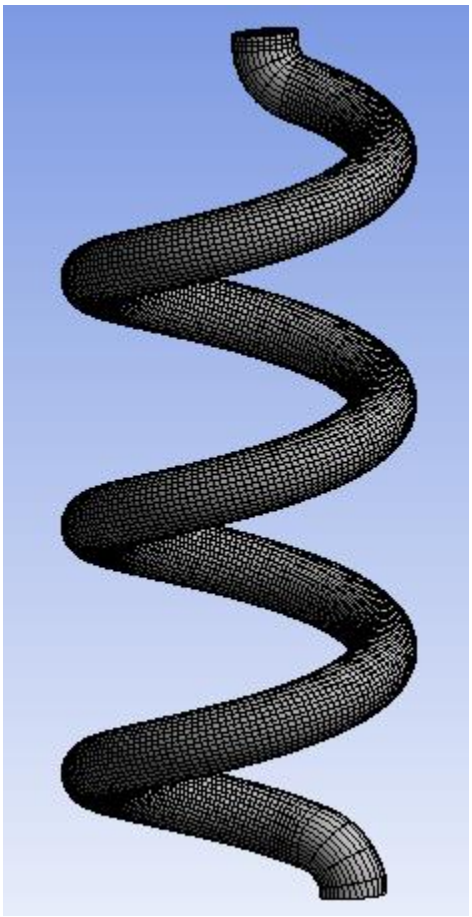

Figure 3.5: Mesh geometry of helical receiver

The mesh cells of our geometries have positive volumes and face and the cells do not intersect with each other. All the surface of the geometry are completely covered by boundary cell faces and all the edges of the geometry are covered by edges of boundary cell faces. In conclusion, we have generated a good mesh to obtain accurate result for our simulations.

For a single part of helical receiver, Table 3.2 shows the number of mesh elements and nodes used. With our computational resource, we cannot exceed number of mesh elements greater than 512000. So, instead of analyzing the total receiver arrangement, we have analyzed a single part of the receiver system.

Table 3.2: Height and arc length of receivers

Receiver	No of Nodes	No of Elements
R3	1255594	420742
R4	1168734	286559
R5	234177	142141

Another approach of the modeling was also introduced. Here, the receiver was considered to be placed in a zone of air. The helical receiver was contained in a box cavity and the cavity space was filled with incompressible air. Following figure 3.6 shows the geometry outline, mesh on the box surface and mesh at section.

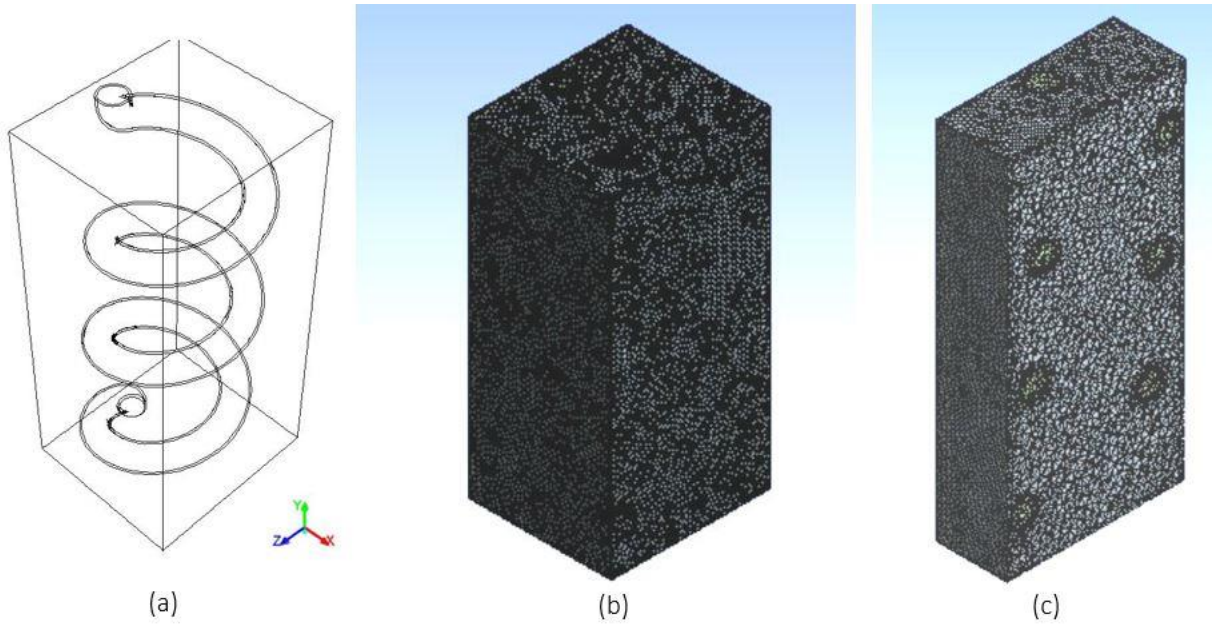

Figure 3.6: (a) Geometry of helical receiver in a zone of air, (b) Mesh at air zone wall surface, (c) Mesh at cross section

As we can see in figure 3.6, more mesh element were necessary for this approach. About 1 million mesh elements were required to generate the mesh shown. In the mesh at cross section, we observe more dense mesh around the receiver.

3.3 COMPUTATIONAL MODELING

3.3.1 Single Phase Model

A vertical tubular receiver is designed similar to the dimension of the existing experimental and numerical setup from [29]. The receiver is analyzed numerically and result is compared for validation of our numerical setup. The vertical receiver is 1 m high with tube thickness 2 mm and outer diameter 20 mm [29].

A vertical receiver of height 600 mm with tube thickness 3 mm and outer diameter 46 mm is designed to compare with helical receivers. This is done to reduce the number of mesh elements in calculation. Three other receivers are designed with the same height to compare results and analyze performance. Helical tubular solar receivers with tube thickness 3 mm, height 600 mm and outer tube diameter 46 mm are designed. One of them has two rotations, another of them has three rotations and the other one has two rotations with outer tube diameter 30 mm for observing the change in performance with varying tube diameter and helix rotations.

For all the single phase models, alloy625 is used as tube material and molten salt is used as the heat transfer fluid. For molten salt, density, thermal conductivity and specific heat capacity are supposed to be constant $8440\ kg/m^3$, 0.571 W/m.K and 1510 J/kg.K respectively [29]. Wall heat conduction is considered. Alloy625 is a Nickel-Chromium alloy for high strength, excellent fabrication ability and outstanding corrosion resistance at very high temperature with density $8440\ kg/m^3$, thermal conductivity 16.3 W/m.K and specific heat capacity 505 J/kg.K [29]. For the test case with supercritical CO_2, density $104.18\ kg/m^3$ and 1268 J/kg.K heat capacity is considered [33].

A radiation model is considered to be most suitable for our setup, because the major heat source is concentrated solar radiation. Among radiation models, Discrete Transfer Radiation Model (DTRM) neglects scattering and emissivity and only Discrete Ordinate (DO) model allows specular reflection and calculation of radiation in semi-transparent media. So, we have used the discrete ordinate radiation model to analyze performance of our receivers. The DO radiation model is enabled through several steps. At first, DO radiation model is turned on.

Energy equation will be automatically turned on. Material properties for heat transfer fluid and tube are defined for the model. Then, radiation boundary conditions are defined. UDF for distributed heat flux boundary condition is loaded. Least squares cell based gradient is used for spatial discretization. Flow, turbulence, energy and discrete ordinates equations are solved.

For a defined position, the radiative heat transfer equation is used for an absorbing, emitting and scattering medium with a vector direction $\vec{s}$ considering the global Cartesian system (x,y,z). The discrete ordinate (DO) radiation model used this radiative transfer equation to solve for a finite number of discrete solid angles for a defined problem. The number of rays controls the fineness of the angular discretization. The equation 2 is as follows

$$\nabla.(I(\vec{r},\vec{s})\vec{s}) + (a+\sigma_s)I(\vec{r},\vec{s}) = an^2\frac{\sigma T^4}{\pi} + \frac{\sigma_s}{4\pi}\int_0^{4\pi} I(\vec{r},\vec{s}')\Phi(\vec{s}\,\vec{s}')d\Omega' \qquad (2)$$

where, n is the refractive index, I is the irradiance, σ is the stephen-boltzman constant.

3.3.2 Multiphase Model

Receivers used in the single phase model are used for the multiphase model. Alloy635 material is used for tube material, and mixture of alumina particle and air is used as heat transfer fluid. Alumina is used as primary phase and air as secondary phase.

Multiphase flows where two phases exist but are not chemically related are very common, and several types of models are found relative to this system. Discrete Phase Model (DPM), Eulerian Multiphase Model, Mixture Model, Volume of Fluid Model, Porous Media Model are all basic models of multiphase flows [34]. Among these models, for gas-solid pneumatic transport flow system, Mixture model with homogeneous flow and Eulerian granular model are recommended in the Ansys Fluent user guide [34]. Mixture model has some limitations. So, Eulerian granular model for multiphase flow is considered for our simulation.

Systems of mass, momentum and energy equation are solved for each phase. Two phases are coupled. Considering plug flow, laminar model is used for dispersed flow of solid particle in air. Air is used as the primary phase. Alumina [7] solid particles are used as the secondary phase. Gravitational acceleration 9.81 m/s is applied in the negative y-direction.

The conservation equation of mass is

$$\frac{\partial}{\partial t}(\alpha\,\rho) + \nabla.(\alpha\,\rho\,u) = 0 \qquad (3)$$

The conservation equation of momentum for gas phase is

$$\frac{\partial}{\partial t}(\alpha_g \rho_g \vec{u}_g) + \nabla.(\alpha_g \rho_g \vec{u}_g \vec{u}_g) = -\alpha_g \nabla p + \nabla.\bar{\bar{\tau}}_g + \alpha_g \rho_g \vec{g} + K_{sg}(\vec{u}_s - \vec{u}_g) \quad (4)$$

The conservation equation of momentum for solid phase is

$$\frac{\partial}{\partial t}(\alpha_s \rho_s \vec{u}_s) + \nabla.(\alpha_s \rho_s \vec{u}_s \vec{u}_s) = -\alpha_s \nabla p - \nabla p_s + \nabla.\bar{\bar{\tau}}_s + \alpha_s \rho_s \vec{g} + K_{gs}(\vec{u}_g - \vec{u}_s) \quad (5)$$

Gas-solid momentum exchange co-efficient,

$$K_{gs} = K_{sg} \quad (6)$$

Stress-strain tensor is given by

$$\bar{\bar{\tau}}_i = \alpha_i \mu_i \left(\nabla \vec{u}_i - \nabla \vec{u}_i^{\,T}\right) + \alpha_i \left(\lambda_i - \frac{2}{3}\mu_i\right) \nabla.\vec{u}_i \bar{\bar{I}}$$

The compressibility effect of air is neglected and hence the bulk viscosity is assumed to be zero.

3.4 BOUNDARY CONDITIONS

In single phase, one side of the receiver is open to incoming heat flux radiation. Heat flux on heating surface is according to the following function for modeling a more practical approach.

$$q(\theta) = q_{net} cos\theta \qquad (-90^o \leq \theta \leq 90^o) \quad (7)$$

Molten salt is used as heat transfer fluid. Inlet temperature of molten salt is considered to be 523 K with inlet velocity 0.5 m/s at atmospheric pressure. Incoming heat flux is considered to be 400,000 W/m^2. This distributed heat flux is applied in Ansys Fluent using a user-defined function written in the C programming language. The code is as follows

```
#include "udf.h"
DEFINE_PROFILE(heat_flx, thread, position)
{
real x[ND_ND];
face_t f;
real qmax, qmin;
qmin = 0;
qmax = 400000;  //net heat flux
xmax = 0.02277944;      //maximum x-coordinate
  begin_f_loop(f, thread)
    {
      F_CENTROID(x,f,thread);
        if(x[0] > -9.80087e-05)
      F_PROFILE(f, thread, position) = (qmax-qmin)*cos(90*(xmax-x[0]));
    }
  end_f_loop(f, thread)
}
```

In multiphase modeling, alumina (Al_2O_3) is used as falling particle of diameter 0.5-1 mm, spherical shaped. Receiver wall outer surface temperature is considered 523 K-800 K variable temperature throughout the heating surface. Inlet temperature of 523 K for both phases is considered. Inlet velocity 0.5 m/s is used for both air and solid particle.

For the receiver in a box of air, constant heat flux is applied on one side of the box because in practical approach, major part of the radiation is coming from one direction. Heat flux is passing through the air zone to reach the surface of the receiver. Applied solar radiation needs to pass through more area to reach the behind part of the receiver than the front part. So, surface temperature on the behind part of the receiver will be comparatively low.

For the receiver model placed in a rectangular box of air zone, all inlet boundary conditions are considered same as before. However, applying the heat flux was done with different approach. Instead of using a user-defined function in fluent, constant heat flux of same magnitude was applied on one side of the air zone wall. The reason for this is that the major portion of radiation is coming from one side of the receiver due to the motion of the sun and the fixed heliostats.

3.5 SOLUTION METHODS

Phase coupled simple scheme is used for multiphase flow. Least square cell based gradient with second order upwind momentum, volume fraction, and dissipation rate is used for spatial discretization. Flow, volume fraction and energy equations are solved in commercial software Fluent.

Chapter 4: Result & Discussion

In our study, five tubular receivers for solar tower have been observed to find a novel high temperature receiver design for improvement of performance of overall solar tower system. Heat transfer fluid flow at steady state has been considered through different receivers and performances are analyzed numerically with commercial software Ansys FUENT 15.0. For fluid flow thorough the receivers, single phase modeling approach has been introduced and for solid particle flow through receivers, multiphase modeling approach has been introduced. The solid particle flow is a solid-gas pneumatic transport plug flow. That is why both single and multiphase modeling approaches are used. Pressure based solver is used in both single and multiphase modeling approach.

4.1 Numerical Results

For all the receivers, same boundary conditions have been used to analyze the performance in order to obtain the novel high temperature receiver design. Energy supplied to the receiver is through the concentrated heat flux coming from the heliostats. So, we applied a net heat flux coming from one side of the receiver and distributed throughout the surface of the receivers. Because of the distributed heat flux, distributed temperature profiles have been observed throughout the surface of the receivers. After applying the boundary condition, temperature profile at tube surface is shown in Figure 4.1.

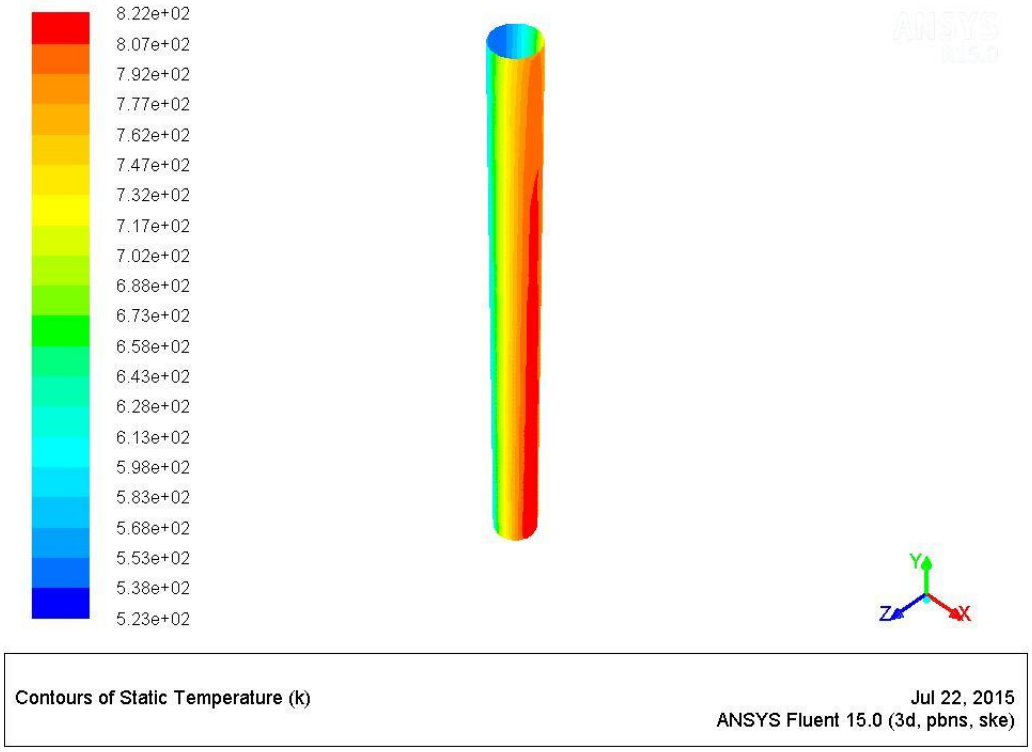

Figure 4.1: Temperature profile at tube outer surface of receiver 2

Observing figure 4.1, surface temperature gradually decreases along the height and also along the diameter. The reason behind this is that at inlet the HTF has lower temperature than at near outlet. So, the temperature difference between wall and HTF is higher near inlet than outlet. According to fluid dynamics, we will obtain higher heat transfer with higher temperature difference.

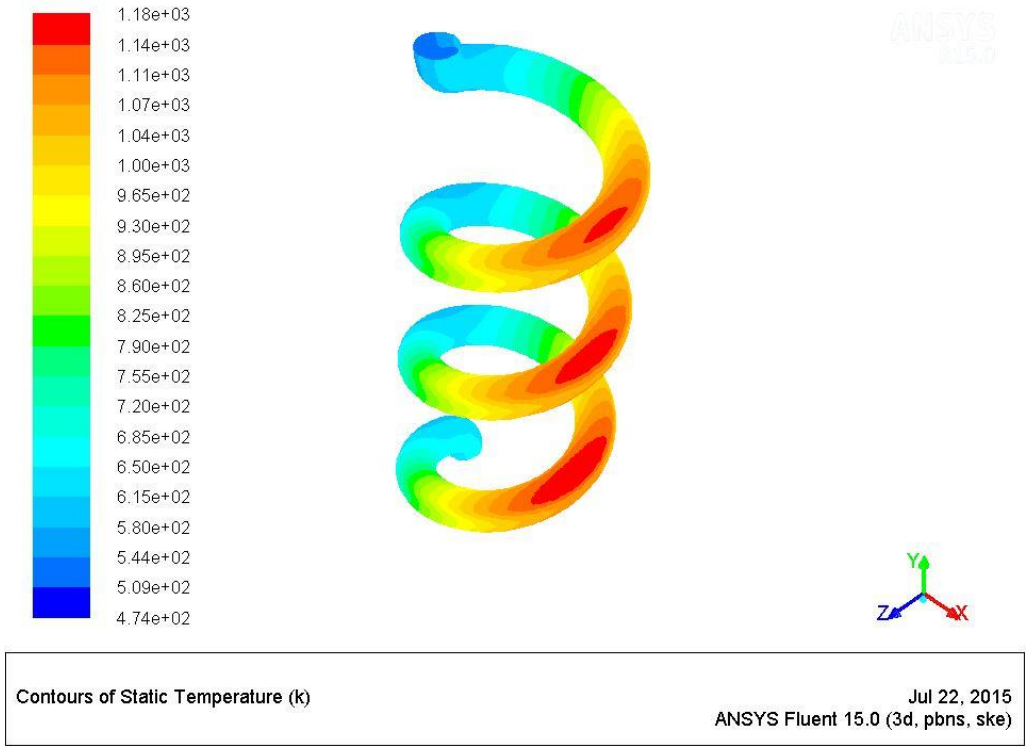

Figure 4.2: Temperature profile at tube outer surface of receiver 3

Temperature profile of helical receiver surface is shown in figure 4.2 with the same boundary condition, tube diameter and tube thickness and vertical height. Higher temperature is achieved at receiver surface for the helical receiver. For the vertical receiver, heat transfer fluid near hot wall mostly absorbs the heat energy but in helical receiver, the fluid mixing is more often and resident time is much higher. That leads to obtaining higher temperature of tube surface at area directly exposed to the incoming radiation. There is a higher heat loss on the back side of the helical receivers. It is due to having greater surface area than the vertical receivers.

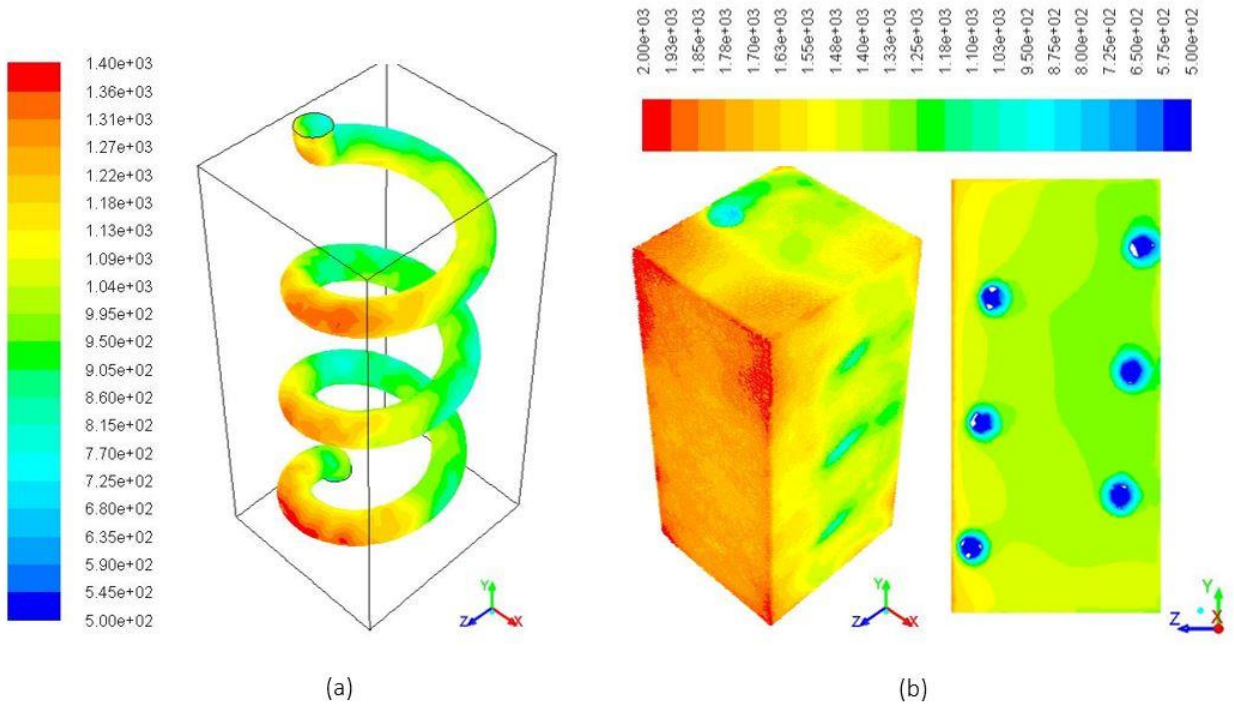

Figure 4.3: (a) Surface temperature contour of receiver 3 in a box of air zone, (b) Temperature contour at wall surface of air zone and cross-section

Result for modeling of helical receiver in a box of air zone is shown in figure 4.3. We observe that temperature contour is similar to the temperature contour shown in figure 4.2 for receiver 3. We have higher heat loss on the behind part of the helical receiver. From the cross-section, we observe that temperature is gradually decreasing throughout the z axis. Although this approach is closer to a practical approach, it requires very high number of mesh elements. Due to limitation of our computational resources, we decided to follow the application of heat flux with the user-defined function for our study.

We observe the pressure and velocity contour of HTF passing through receiver 1 in figure 4.4. Here, the pressure is gradually decreasing from inlet to outlet. The reason for this phenomenon is that we considered a forced constant inlet velocity for HTF. Due to this boundary condition, pressure is comparatively high near inlet and gradually decrease throughout y-axis. As for velocity, we observe that velocity is higher near mid-section. This is due to the viscous force of HTF acting near receiver wall.

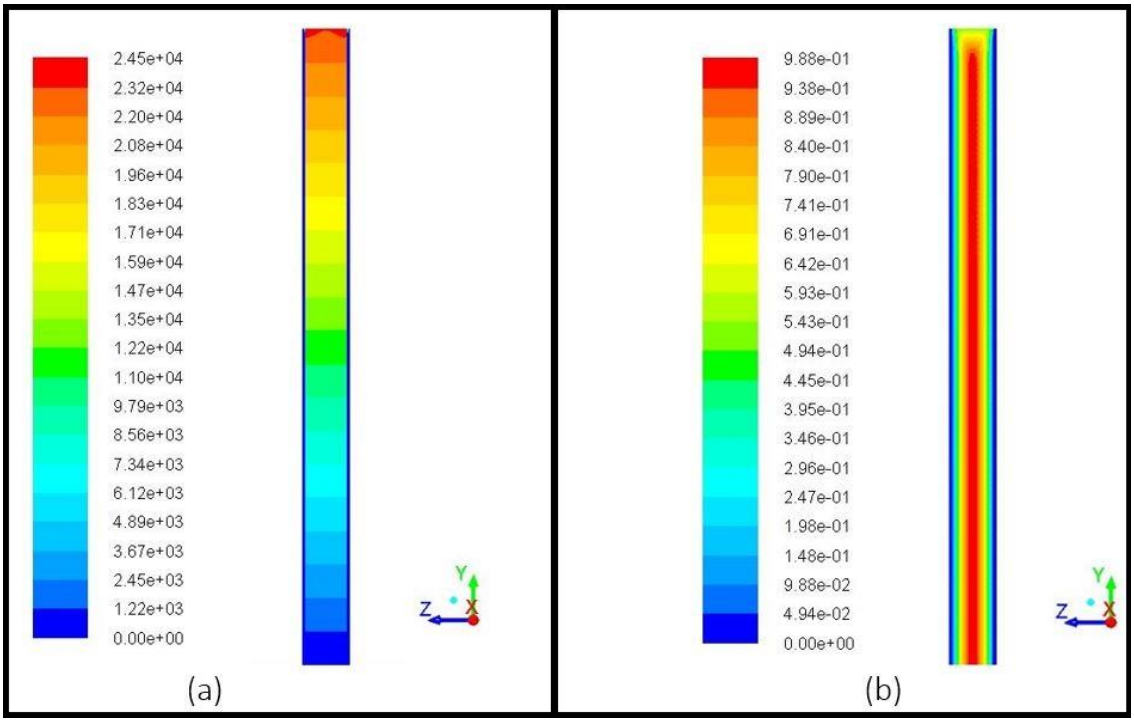

Figure 4.4: (a) Pressure contour for receiver 1, (b) velocity contour for receiver 1

Temperature at different path lines are shown in figure 4.5. We observe that at the same y-axis position, different path line may have different temperature. This is due to the application of heat flux from one side of the receiver and the mixing of HTF while flowing from inlet to outlet. For all the path lines shown, temperature is gradually increasing from inlet to outlet.

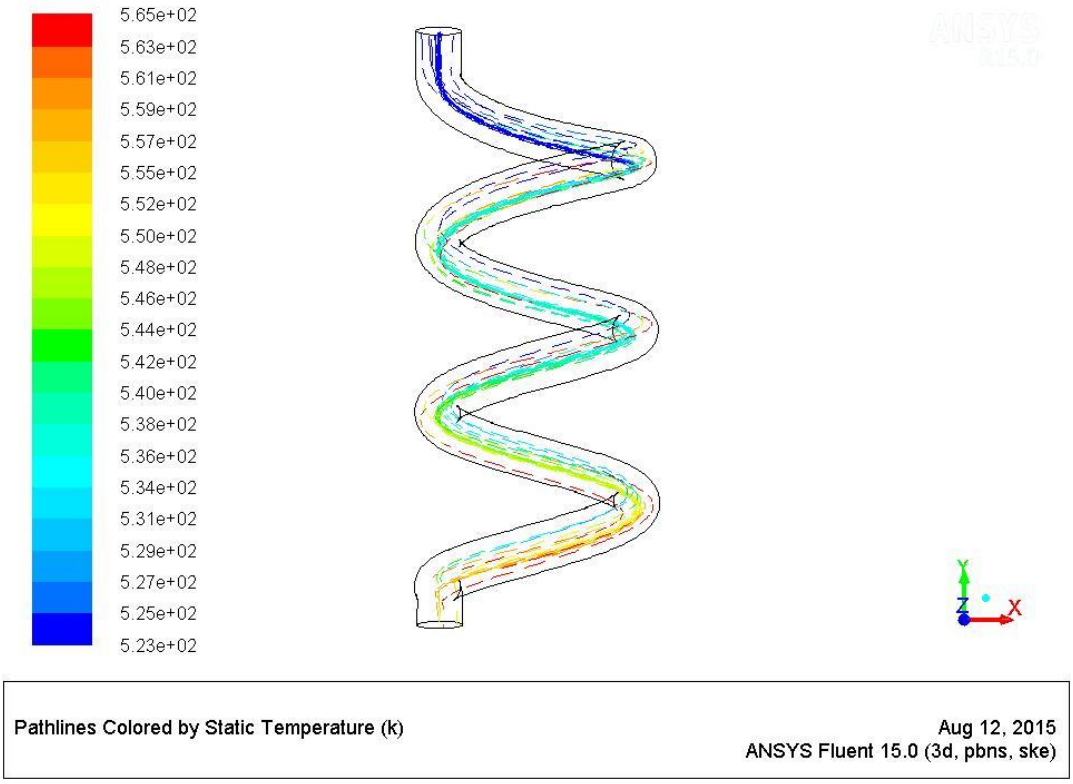

Figure 4.5: Temperature profile of HTF at different path lines for receiver 1

4.1.1 Single Phase

The receivers have been sliced at equidistant points along vertical height and average temperature of HTF is calculated at those sections to obtain an overview of the change of average temperature of HTF throughout the receivers. Figure 4.6 shows a graphical representation of the sliced HTF domain along the vertical height of receiver 1. Average temperature is calculated at each of those sections to observe the temperature rise and also the temperature distribution at the sections. We observe in figure 4.6 that in one region HTF obtains a high temperature while in other region it has low temperature. This may cause HTF like molten salt become unstable. Because from our previous study, we discussed that molten salt becomes unstable operation at higher than $600^{o}C$.

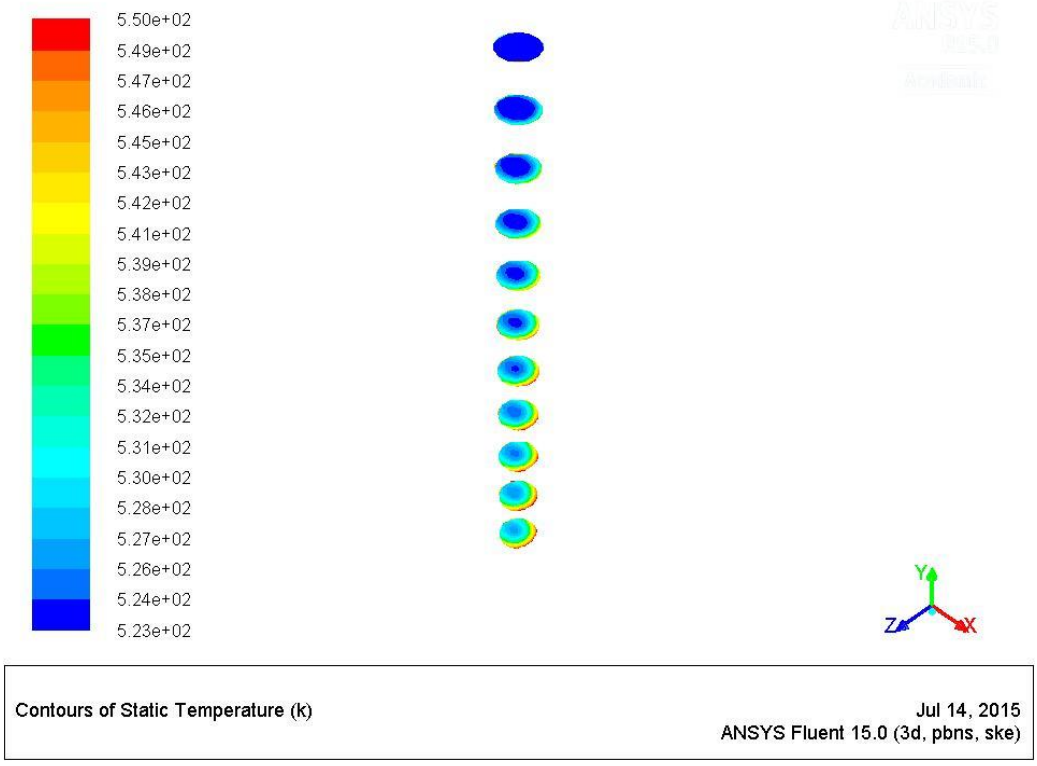

Figure 4.6: Temperature profile of HTF at different sections of receiver 1

Receiver 1 is used for validating our modeling approach. Figure 4.7 shows temperature rise in receiver 1 near the closest surface exposed to heat flux. Temperature is gradually increasing from inlet to outlet. This is due to higher temperature difference between tube wall and HTF near inlet than outlet. According to heat transfer in fluid dynamics, higher transfer occurs with higher temperature difference.

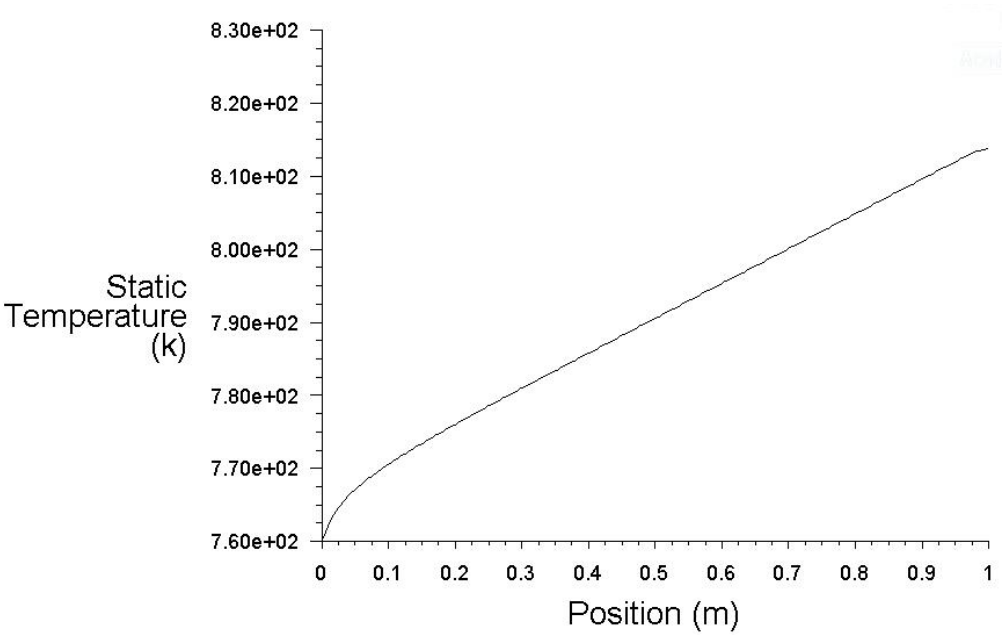

Figure 4.7: Temperature vs y-axis position near closest surface exposed to heat flux of receiver 1

According to the numerical and experimental setup for this tube dimension and boundary conditions [29], temperature of the outer wall of the heating surface increases from 788 K to 822 K. In our case, we have temperature rise from approximately 760 K to 818 K. The error considered between 822K and 818 K is less than 0.05% and the error between 788 K and 760 K is 3.5%. The temperature rise near inner wall is shown in figure 4.8.

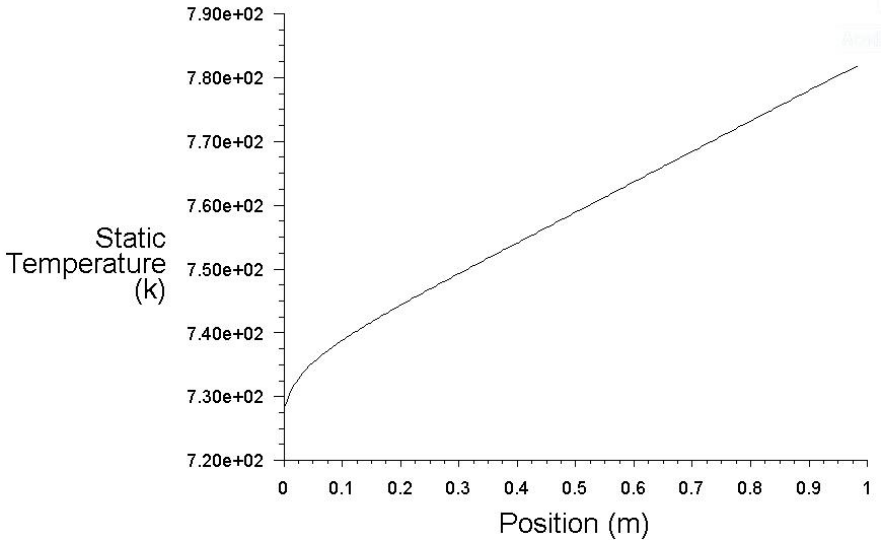

Figure 4.8: Temperature vs y-axis position near inner wall of receiver 1

In figure 4.7, we observe that along y-axis, temperature is varying from about 729 K to 784 K. This is the temperature rise at inside the wall thickness. Compared to the outer wall, the inside wall has lower temperature at inlet and outlet. In conclusion, due to the thickness, temperature drops.

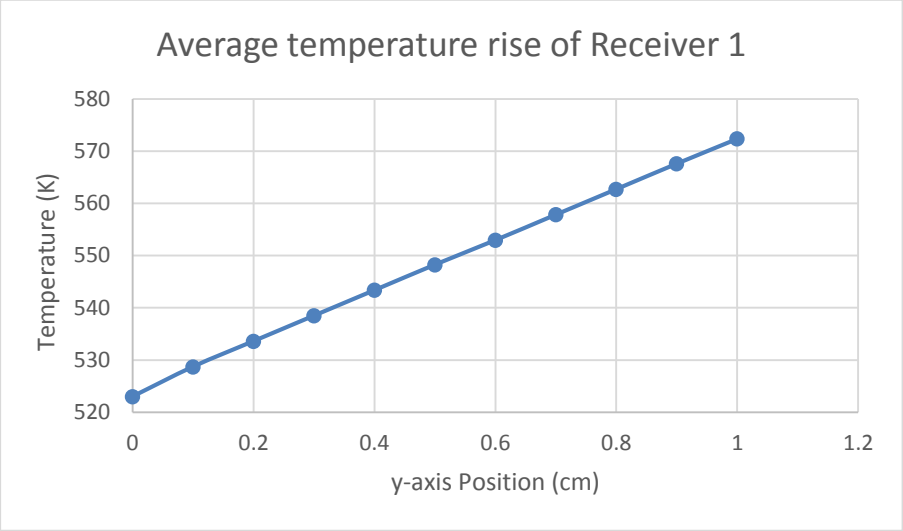

Figure 4.9: Average temperature vs y-axis position of receiver 1

Average fluid temperature throughout receiver 1 along the height is shown in Figures 4.9. The receiver has been sliced along x-z axis at equidistant positions and average temperature data has been collected to plot an average temperature profile along y-axis.

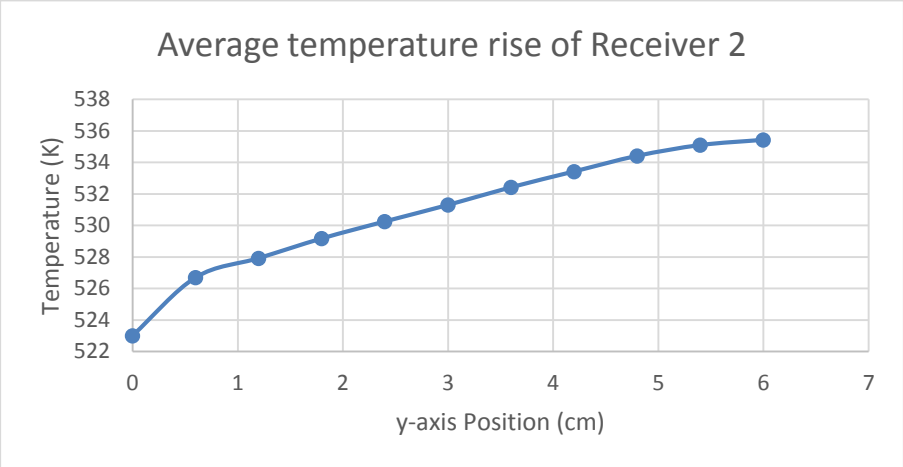

Figure 4.10: Average temperature vs y-axis position of receiver

According to figure 4.10, average temperature is gradually increasing throughout the height for receiver 2. The outlet average temperature obtained is around 535 K in one cyclic operation.

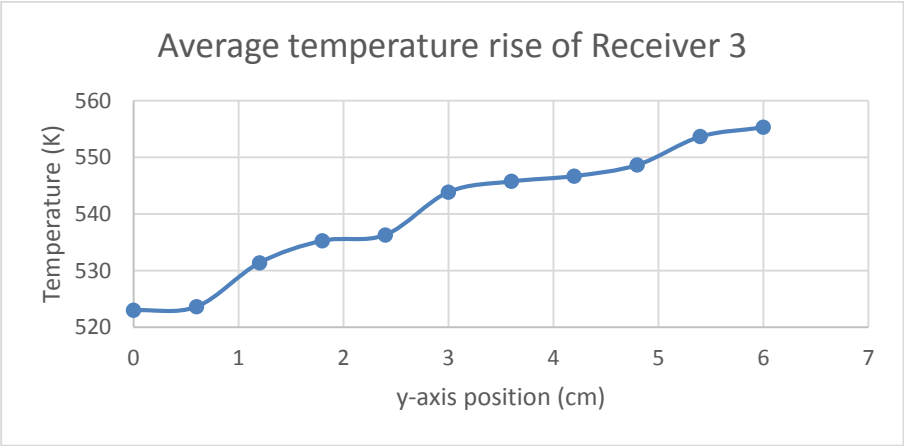

Figure 4.11: Average temperature vs y-axis position of receiver

According to figure 4.11, average temperature is gradually increasing throughout the height for receiver 3. At some region of the plot, temperature rise is almost none due high heat loss. This happens when the HTF moves on the back side of the receiver, where we have very low heat flux. This happened for all the helical receivers.

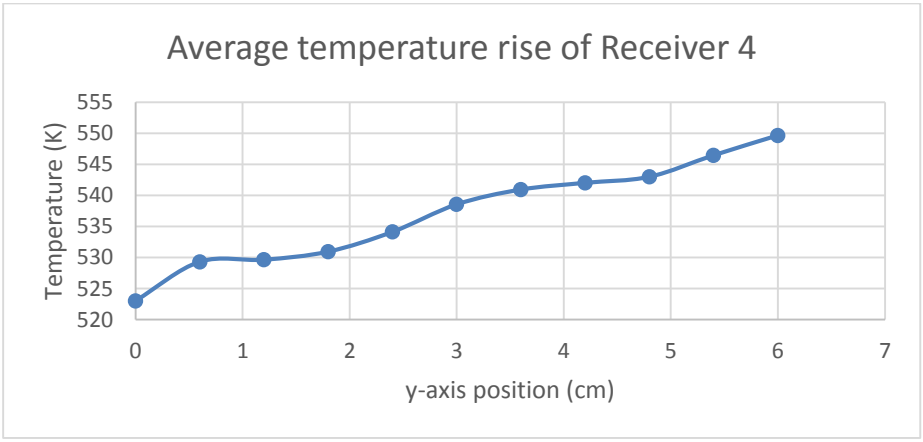

Figure 4.12: Average temperature vs y-axis position of receiver

According to figure 4.12, average temperature is gradually increasing throughout the height for receiver 4. It has a lower outlet temperature comparing to figure 4.11. It is due to reduction of number of rotation or the increase in pitch.

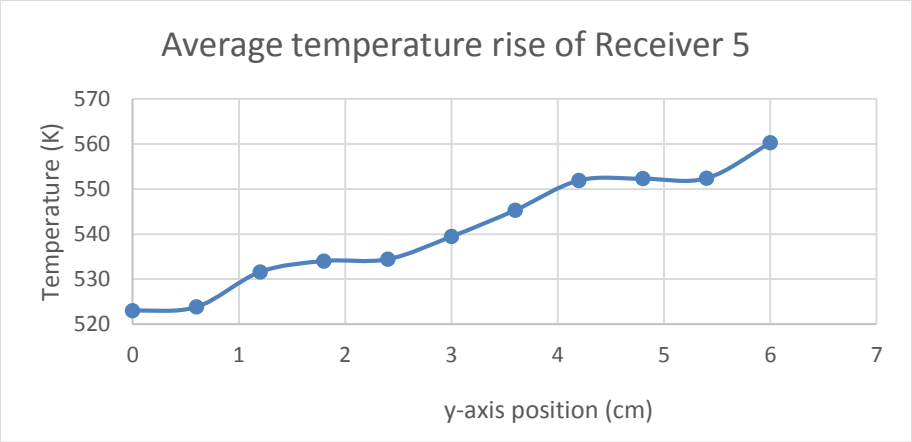

Figure 4.13: Average temperature vs y-axis position of receiver

According to figure 4.13, average temperature is gradually increasing throughout the height for receiver 5. It has a higher outlet temperature comparing to figure 4.12. It is due to reduction in tube diameter.

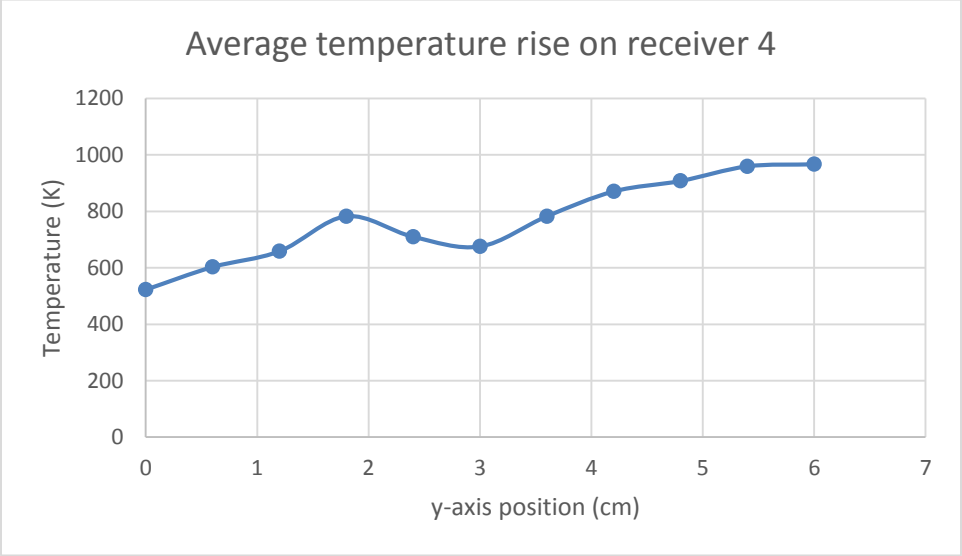

Figure 4.14: Average temperature vs y-axis position of receiver 4 for supercritical CO_2

According to figure 4.14, average temperature is gradually increasing throughout the height for receiver 4. It has a higher outlet temperature comparing to figure 4.12. It is due to considering supercritical CO_2, instead of using molten salt. Due to the thermal properties of supercritical CO_2, better performance can be achieved.

4.1.2 Multiphase

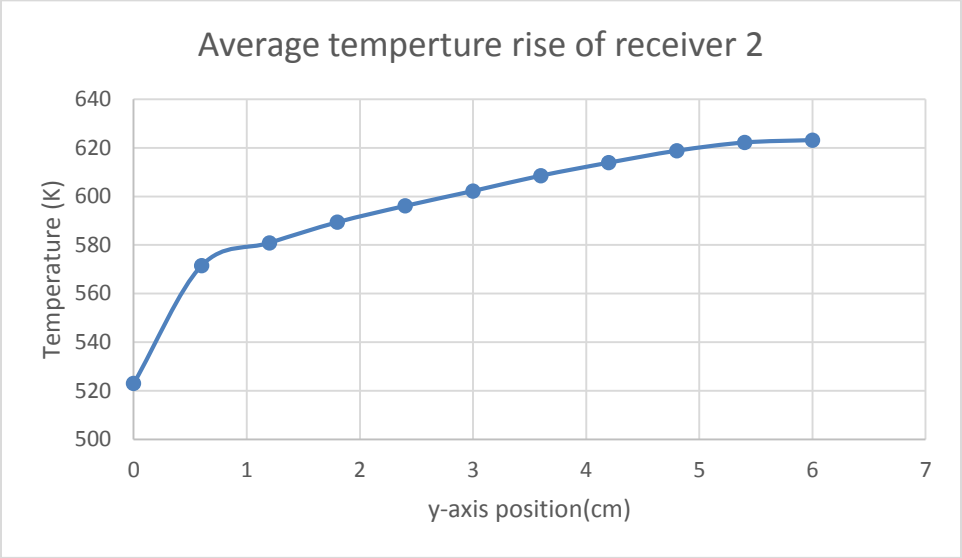

Figure 4.15: Average temperature vs y-axis position of receiver 2

According to figure 4.15, average temperature is gradually increasing throughout the height for receiver 2. This is similar to single phase model.

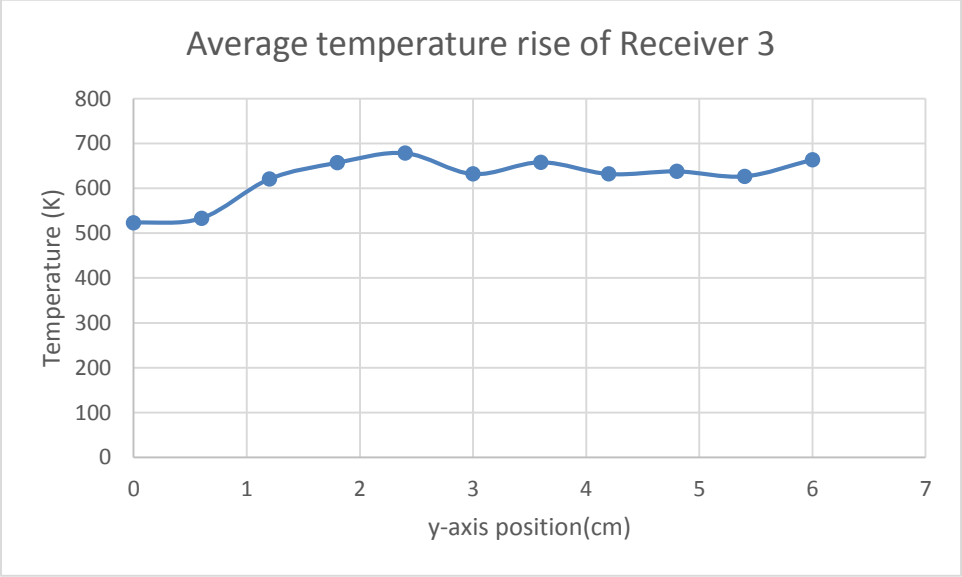

Figure 4.16: Average temperature vs y-axis position of receiver 3

According to figure 4.16, average temperature is gradually increasing throughout the height for receiver 3. At some region of the plot, temperature rise is almost none due high heat loss. This happens when the HTF moves on the back side of the receiver, where we have very low heat flux. This happened for all the helical receivers.

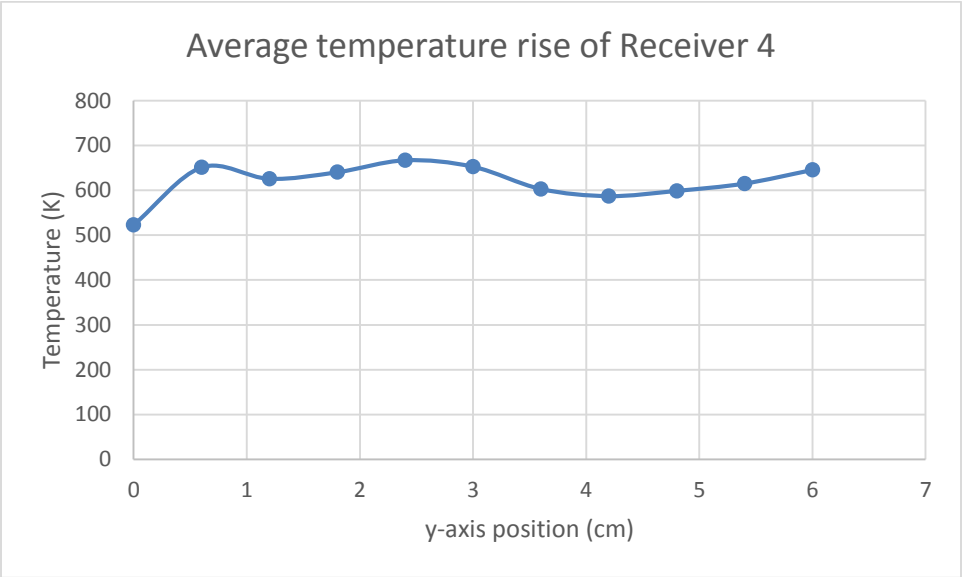

Figure 4.17: Average temperature vs y-axis position of receiver 4

According to figure 4.17, average temperature is gradually increasing throughout the height for receiver 4. It has a lower outlet temperature comparing to figure 4.16. It is due to reduction of number of rotation or the increase in pitch.

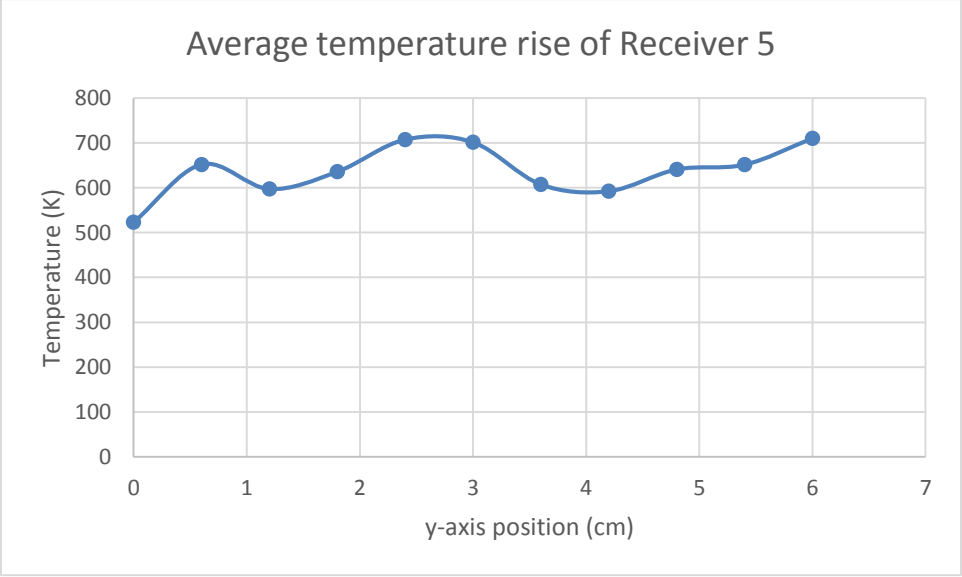

Figure 4.18: Average temperature vs y-axis position of receiver 5

According to figure 4.18, average temperature is gradually increasing throughout the height for receiver 5. It has a higher outlet temperature comparing to figure 4.17. It is due to reduction in tube diameter.

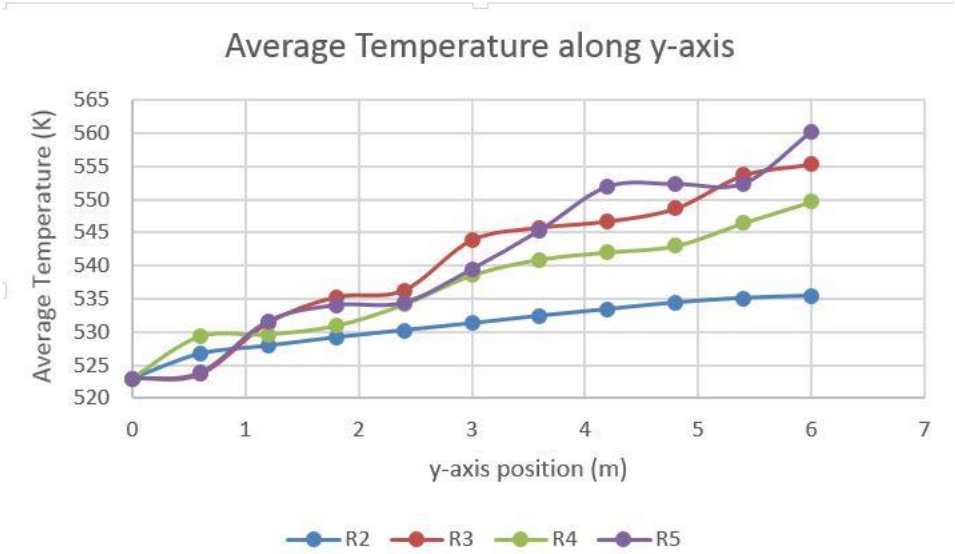

Figure 4.19: Average temperature comparison in single phase

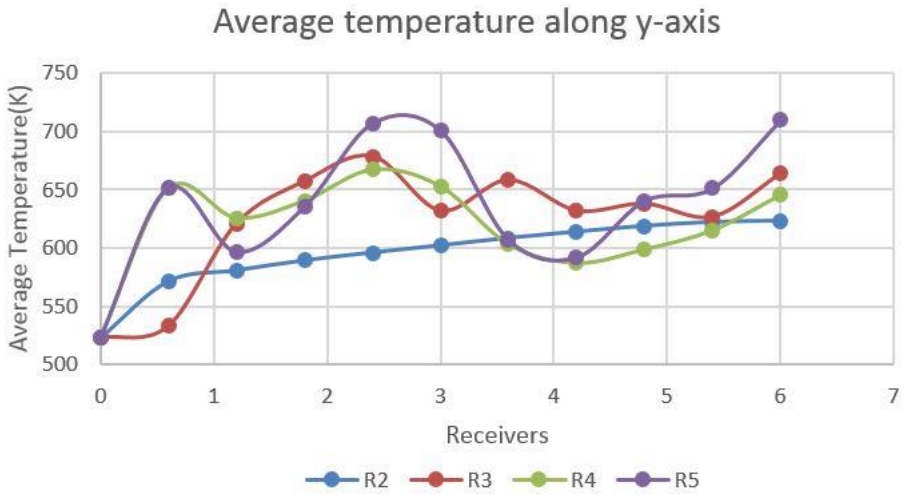

Figure 4.20: Average temperature comparison in multiphase

Average temperature comparison is shown for single and multiphase in figure 4.19 and figure 4.20. As we can observe, R2 is the vertical receiver and has the lowest average outlet temperature. R3 has three rotations and R4 has two rotations. With reduced number of rotations, average outlet temperature drops. However, with reduction of tube diameter in R5, temperature gain increases. Average temperature variation is similar for both single and multiphase model. In

multiphase model, higher temperature gain is achieved because of considering alumina particle, which has higher heat capacity than molten salt. A bar plot of outlet temperatures of the receivers are plotted for both single and multiphase models in the following figures 4.21 and 4.22 to show the change in performance of the receivers graphically.

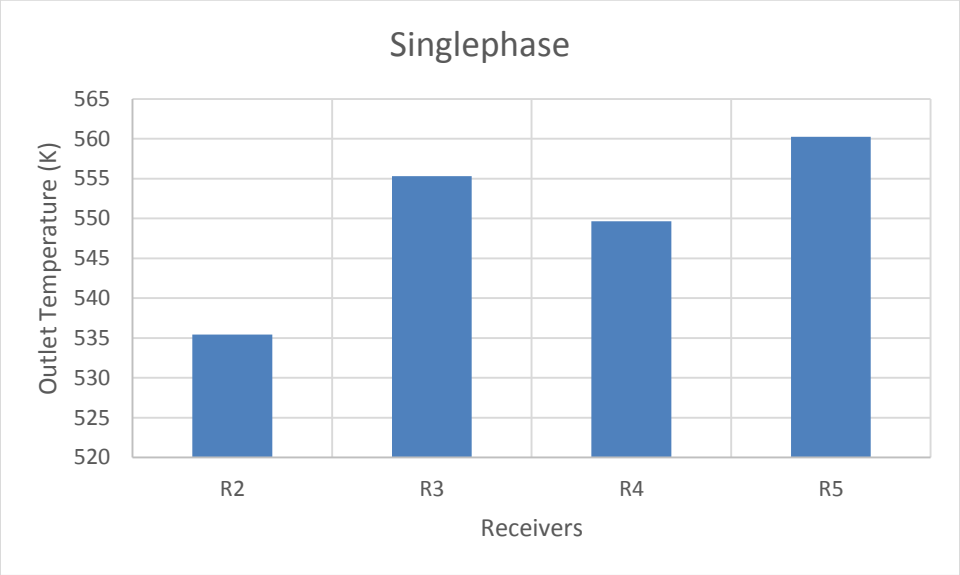

Figure 4.21: Outlet temperature bar chart of receivers (Single phase)

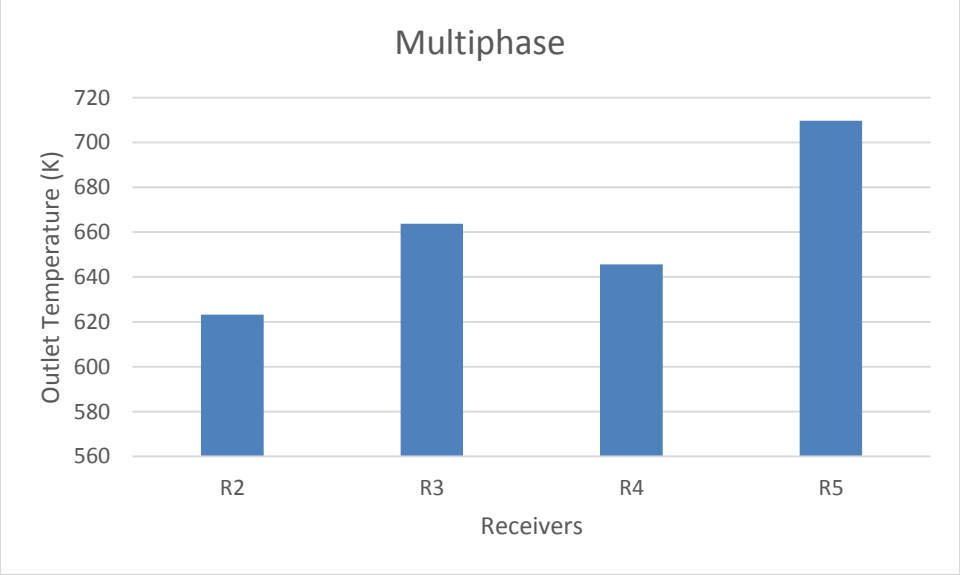

Figure 4.22: Outlet temperature bar chart of receivers (Multiphase)

4.2 EFFICIENCY CALCULATION

Efficiency of receiver is calculated using total energy supplied and heat losses. Considering 0.85 emissivity, efficiency is calculated using following formulas [33].

Convective heat loss, $Q_{conv} = h_{air} A_s (T_w - T_\infty)$ (8)

Radiative heat loss, $Q_{rad} = \varepsilon \sigma A_s ({T_w}^4 - {T_\infty}^4)$ (9)

Reflective heat loss, $Q_{refl} = (1 - \alpha) Q_{sun}$ (10)

Total heat loss, $Q_{loss} = Q_{conv} + Q_{rad} + Q_{refl}$ (11)

Heat supplied, $Q_{in} = q \times A_s$ (12)

Efficiency, $\eta_{th} = \frac{Q_{in} - Q_{loss}}{Q_{in}} \times 100\%$ (13)

Here, T_w is wall outside temperature, T_∞ is ambient temperature and ε is the emissivity considered.

Table 4.1: Receiver performance single phase

Receiver	Outlet temp (K)	Heat loss (W)	Efficiency(%)	Avg Temp rise
R2	535.43	1172.8	93.23	12.43
R3	555.29	8462.6	87.76	32.29
R4	549.65	7298.3	84.75	26.65
R5	560.25	3804.5	87.09	37.25

Observing table 4.1, we see that R2 has a higher efficiency. This is higher because we only considered one vertical tube. Helical receivers have 200 mm helix diameter so that it is covering a large area and thus on the back side of the helical receiver temperature is comparatively low. For simplifying the modeling, we considered a single part of the receiver.

The vertical tubes on the back side will have very low efficiency and the front vertical tube closest to radiation will have highest efficiency calculated and overall receiver efficiency will be less than 93.23%. Observing R3, R4 and R5 from table 4.1, we see that efficiency increases with reduction of tube diameter. The outlet temperature of supercritical CO_2 is found as 967.135 K. However, proper stress analysis needs to be done for supercritical CO_2 because in very high temperature, it generates a very high pressure, 20 MPa [33].

Chapter 5: Conclusion

The primary goal of this study was to design a novel high temperature solar tower receiver for both heat transfer fluid and solid particle. Among the solid particle receivers, all of them considers vertical free fall to utilize the gravitational force but we have analyzed that twisting the path of the vertical free fall will lead to an increase in residence time and thus higher temperature gain in one cycle.

While using molten salt in solar tower, heat transfer fluid near high wall temperature will achieve very high temperature compared to the other part of the fluid zone. However we cannot allow molten salt to achieve more than 600^oC for stability. For the inclined angle in helical receiver, heat transfer fluid will mix and transfer heat to nearest region more evenly than vertical free fall. This reduces the possibility of obtaining very high temperature at one region and very low temperature at other region of heat transfer fluid.

Observing figures 4.15 and 4.16 and comparing R2 and R3, we can conclude that receiver performance increases for helical receiver compared to a vertical receiver of the same height. Also, comparing R3 and R4, we observe that receiver performance decreases with reduction of number of rotations of a helical receiver. We need to consider incident angle more than 30^o, when we are using free falling solid particle. Again, if we reduce the tube diameter, comparing R4 and R5, we observe decrease in performance. However, we need to have a proper inner diameter with respect to particle size to avoid blocking inside tube.

While considering supercritical CO_2 as HTF, very high internal pressure (around 20 MPa) will develop at high temperature. Our designed helical receiver do not have any sharp edges like the serpentine receiver discussed. In total receiver arrangement, helical tubes will support one another while in contact with each other according to mechanics of materials. This will allow it

to operate in a high internal stress condition with reduced thickness. Also, helical receiver is applicable for both fluid and solid particles.

Chapter 6: Future Work

For the future work, we may use several helical receivers together to have high mass flow rate of heat transfer fluid and also reduce heat loss. The following figure 6.1 shows the geometry of such a case. This way, we can also control incident angle. We may also remove the gap in between the receivers, which may give the receiver more structural stability. When we will consider supercritical CO_2 athe s heat transfer fluid, we may have a very high pressure for high temperature operation. Then structural stability may be considered as a key factor. We can have distributor at inlet and outlet to have uniform flow through receiver.

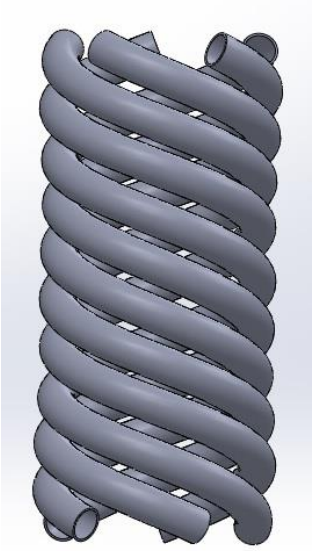

Figure 6.1: Receiver for solar tower

We can experiment on a single helical receiver in small scale and compare data with numerical results to have strong validation of our modeled receiver. Also, we may consider different coating materials like Pyromark 2500, to improve incident solar radiation absorption in order to improve overall efficiency. We may change heat transfer fluid and receiver material to observe performance of the receiver in order to find more potential heat transfer fluid and receiver material. Comparison of performance with different particle sizes may be analyzed. Shadow effect may be considered for more accurate and realistic results.

Also, we are planning to design a tubular volumetric receiver for supercritical CO_2. As we discussed before, supercritical CO_2 is a very potential HTF due to is properties like intoxic,

abundant and operating at a very high temperature. We will make the high temperature region of the receiver, porous so that the supercritical CO_2 will have more resident time for heat transfer. We may observer the temperature and pressure with different porosity to find an optimum volumetric receiver for supercritical CO_2.

References

[1] "IPCC Energy Supply." [Online]. Available: https://www.ipcc.ch/pdf/assessment-report/ar4/wg3/ar4-wg3-chapter4.pdf. [Accessed: 04-Aug-2015].

[2] S. Afrin, V. Kumar, D. Bharathan, G. C. Glatzmaier, and Z. Ma, "Computational Analysis of a Pipe Flow Distributor for a Thermocline Based Thermal Energy Storage System," *J. Sol. Energy Eng.*, vol. 136, no. 2, p. 021010, Sep. 2013.

[3] D. Kearney, U. Herrmann, P. Nava, B. Kelly, R. Mahoney, J. Pacheco, R. Cable, N. Potrovitza, D. Blake, and H. Price, "Assessment of a Molten Salt Heat Transfer Fluid in a Parabolic Trough Solar Field," *J. Sol. Energy Eng.*, vol. 125, no. 2, p. 170, May 2003.

[4] C. K. Ho and B. D. Iverson, "Review of high-temperature central receiver designs for concentrating solar power," *Renew. Sustain. Energy Rev.*, vol. 29, pp. 835–846, Jan. 2014.

[5] W. Moomaw, F. Yamba, M. Kamimoto, L. Maurice, J. Nyboer, K. Urama, and T. Weir, "Introduction: Renewable Energy and Climate Change," in *IPCC Special Report on Renewable Energy Sources and Climate Change Mitigation*, 2011, pp. 161–208.

[6] "International Energy Statistics - EIA." [Online]. Available: http://www.eia.gov/cfapps/ipdbproject/IEDIndex3.cfm?tid=90&pid=44&aid=8. [Accessed: 04-Aug-2015].

[7] "Implication of proposed CO2 Emissions Limitations." [Online]. Available: https://www.ipcc.ch/pdf/technical-papers/paper-IV-en.pdf. [Accessed: 04-Aug-2015].

[8] NREL, "2013 Renewable Energy Data Book." [Online]. Available: http://www.nrel.gov/docs/fy15osti/62580.pdf. [Accessed: 25-May-2015].

[9] M. Rajib, M. Arif Ishtiaque Shuvo, H. Karim, D. Delfin, S. Afrin, and Y. Lin, "Temperature influence on dielectric energy storage of nanocomposites," *Ceram. Int.*, vol. 41, no. 1, pp. 1807–1813, Jan. 2015.

[10] H. Karim, M. A. I. Shuvo, M. T. Islam, G. Rodriguez, A. Sandoval, M. I. Nandasiri, A. M. Schwarz, A. Devaraj, J. C. Noveron, M. Vijayakumar, and Y. Lin, "Porous carbon/CeO 2 composites for Li-ion battery application," in *SPIE Smart Structures and Materials + Nondestructive Evaluation and Health Monitoring*, 2015, p. 94390I.

[11] M. Rajib, R. Martinez, M. Shuvo, H. Karim, D. Delfin, S. Afrin, G. Rodriguez, R. Chintalapalle, and Y. Lin, "Enhanced Energy Storage of Dielectric Nanocomposites at Elevated Temperatures," *Int. J. Appl. Ceram. Technol.*, p. n/a–n/a, May 2015.

[12] M. A. I. Shuvo, T.-L. (Bill) Tseng, M. Ashiqur Rahaman Khan, H. Karim, P. Morton, D. Delfin, and Y. Lin, "Nanowire modified carbon fibers for enhanced electrical energy storage," *J. Appl. Phys.*, vol. 114, no. 10, p. 104306, Sep. 2013.

[13] M. A. I. Shuvo, M. A. R. Khan, M. Mendoza, M. Garcia, and Y. Lin, "Synthesis and Characterization of Nanowire-Graphene Aerogel for Energy Storage Devices," in *Volume 6: Energy, Parts A and B*, 2012, p. 1205.

[14] M. A. I. Shuvo, H. Karim, M. Rajib, D. Delfin, and Y. Lin, "Multifunctional composites for energy storage," in *SPIE Smart Structures and Materials + Nondestructive Evaluation and Health Monitoring*, 2014, p. 905808.

[15] M. A. I. Shuvo, M. A. R. Khan, H. Karim, P. Morton, T. Wilson, and Y. Lin, "Investigation of modified graphene for energy storage applications.," *ACS Appl. Mater. Interfaces*, vol. 5, no. 16, pp. 7881–5, Aug. 2013.

[16] M. Mendoza, "Development of lead-free nanowire composites for energy storage applications," *ISRN ...*, 2012.

[17] M. A. I. Shuvo, H. Karim, M. T. Islam, G. Rodriguez, M. I. Nandasiri, A. M. Schwarz, A. Devaraj, J. C. Noveron, M. Vijayakumar, and Y. Lin, "High-performance porous carbon/CeO 2 nanoparticles hybrid super-capacitors for energy storage," in *SPIE Smart Structures and Materials + Nondestructive Evaluation and Health Monitoring*, 2015, p. 94390H.

[18] "IPCC Hydropower." [Online]. Available: http://srren.ipcc-wg3.de/report/IPCC_SRREN_Ch05.pdf. [Accessed: 04-Aug-2015].

[19] "IPCC Wind Energy." [Online]. Available: http://www.ipcc.ch/pdf/special-reports/srren/Chapter 7 Wind Energy.pdf. [Accessed: 04-Aug-2015].

[20] "IPCC Direct Solar Energy." [Online]. Available: http://www.ipcc.ch/pdf/special-reports/srren/Chapter 3 Direct Solar Energy.pdf. [Accessed: 04-Aug-2015].

[21] J. Duffie and W. Beckman, *Solar engineering of thermal processes*. 1980.

[22] A. A.-Z. R.-Y. Karahagopian, "Solar Energy: A Competitor." [Online]. Available: http://almashriq.hiof.no/lebanon/600/610/614/solar-water/unesco/27-28.html. [Accessed: 26-May-2015].

[23] Solarcellcentral, "Concentrated Solar Power." [Online]. Available: http://solarcellcentral.com/csp_page.html. [Accessed: 27-May-2015].

[24] SEIA, "Concentrating Solar Power | SEIA."

[25] "NREL: Concentrating Solar Power Projects - Jülich Solar Tower." [Online]. Available: http://www.nrel.gov/csp/solarpaces/project_detail.cfm/projectID=246. [Accessed: 04-Aug-2015].

[26] "NREL: Concentrating Solar Power Research Home Page." [Online]. Available: http://www.nrel.gov/csp/. [Accessed: 04-Aug-2015].

[27] S. Afrin, J. D. Ortega, V. Kumar, and D. Bharathan, "A Computational Analysis: A Honeycomb Flow Distributor With Porous Approximation for a Thermocline Thermal Energy Storage System," in *ASME 2013 7th International Conference on Energy Sustainability*, 2013, p. V001T03A013.

[28] N. Hossain and S. Afrin, "Numerical Analysis of Total Energy Storage of Nanofluidized Heat Transfer Fluid in Thermocline Thermal Energy Storage System," ... *Energy ...*, 2014.

[29] X. Yang, X. Yang, J. Ding, Y. Shao, and H. Fan, "Numerical simulation study on the heat transfer characteristics of the tube receiver of the solar thermal power tower," *Appl. Energy*, vol. 90, no. 1, pp. 142–147, Feb. 2012.

[30] "SOLIDWORKS Education Edition 2013 - 2014 | SOLIDWORKS." [Online]. Available: https://www.solidworks.com/sw/education/education-edition-2013-2014-overview.htm. [Accessed: 04-Aug-2015].

[31] "ANSYS 15.0 Release Highlights." [Online]. Available: http://www.ansys.com/Products/ANSYS+15.0+Release+Highlights. [Accessed: 04-Aug-2015].

[32] "Formula for the Arc Length of a Helix." [Online]. Available: http://calculus-geometry.hubpages.com/hub/Arc-Length-of-a-Helix-Formula. [Accessed: 22-Jul-2015].

[33] S. Afrin, J. D. Ortega, C. K. Ho, and V. Kumar, "Modeling of a High-Temperature-Serpentine External Tubular Receiver Using Supercritical CO 2," in *Volume 1: Combined Energy Cycles, CHP, CCHP, and Smart Grids; Concentrating Solar Power, Solar Thermochemistry and Thermal Energy Storage; Geothermal, Ocean, and Emerging Energy Technologies; Hydrogen Energy Technologies; Low/Zero Emission Power Plants an*, 2014, p. V001T02A011.

[34] "FLUENT 6.3 User's Guide - 23. Modeling Multiphase Flows." [Online]. Available: https://www.sharcnet.ca/Software/Fluent6/html/ug/node871.htm. [Accessed: 21-Jul-2015].

[35] IEA, "Key World Energy Statistics 2014." [Online]. Available: http://www.iea.org/publications/freepublications/publication/keyworld2014.pdf. [Accessed: 25-May-2015].

[36] S. E. Guide, "Concentrating Solar Power (CSP) Technology." [Online]. Available: http://solareis.anl.gov/guide/solar/csp/. [Accessed: 26-May-2015].

[37] D. E. S. Basics, “Concentrating Solar Power Dish/Engine System Basics | Department of Energy.” [Online]. Available: http://energy.gov/eere/energybasics/articles/concentrating-solar-power-dishengine-system-basics. [Accessed: 26-May-2015].

[38] S. P. T. Tower, “Solar Power Tower.” [Online]. Available: http://lisas.de/projects/alt_energy/sol_thermal/powertower.html. [Accessed: 27-May-2015].

[39] “ASME DC | Journal of Thermal Science and Engineering Applications | Technical Challenges and Opportunities for Concentrating Solar Power With Thermal Energy Storage.” [Online]. Available: http://thermalscienceapplication.asmedigitalcollection.asme.org/Mobile/article.aspx?articleid=1690813. [Accessed: 21-Jul-2015].

[40] “Concentrating Solar Power Thermal Storage System Basics | Department of Energy.” [Online]. Available: http://energy.gov/eere/energybasics/articles/concentrating-solar-power-thermal-storage-system-basics. [Accessed: 21-Jul-2015].

[41] “Suction-recirculation device for stabilizing particle flows within a solar powered solid particle receiver.” 07-Feb-2012.

[42] “Receivers for solar tower.” [Online]. Available: http://sfera2.sollab.eu/uploads/images/networking/SFERA SUMMER SCHOOL 2014 - PRESENTATIONS/SolarTowerReceivers - Bernhard Hoffschmidt.pdf. [Accessed: 23-Jul-2015].

[43] J. D. Ortega, “Design and evaluation of a high temperature/pressure supercritical carbon dioxide direct tubular receiver for concentrating solar power applications,” 2014.

Vita

Nazmul Hossain, son of Delowar Hossain, was born on December 12, 1989 in Bangladesh. He completed his Bachelor in Mechanical Engineering from Khulna University of Engineering & Technology, Bangladesh in 2011. His undergraduate research was on experimental setup of solid desiccant evaporative cooling system. He has gone through industrial training at BITAC, Bangladesh during his undergraduate study. After graduation, he worked in a reputed furniture manufacturing industry for fifteen months as a production officer. He pursued his Masters in Computational Science from year 2013 at University of Texas at El Paso. He has been awarded a COURI summer research assistant program scholarship after competitive evaluation of a submitted proposal. He has been a teaching assistant for several undergraduate and graduate courses and also been a tutor on Mathematics Resource Center for Student (MaRCS). His Masters research is related to Concentrating Solar Power (CSP) receiver and heat transfer fluid. He has been an author and co-author of conference papers published including American Society of Mechanical Engineers (ASME) International Conference on Energy Sustainability, and the Southwest Energy Science and Engineering Symposium.

Permanent address: 300 W Nevada Ave. Apt 3
El Paso, Texas, 79902

This thesis/dissertation was written by Nazmul Hossain